UCL Université catholique de Louvain

École polytechnique de Louvain (EPL)

Photocatalytic degradation of anti-cancer drugs

Dissertation presented by
Maël MAKOUDI

for obtaining the Master's degree in
Chemical and Materials Engineering

Supervisor(s)
Patricia LUIS ALCONERO, Raphaël JANSSENS

Reader(s)
Iwona CYBULSKA, Denis DOCHAIN

Academic year 2017-2018

Abstract

Antineoplastic drugs are compounds used as anti-cancer treatment. Their toxicity is an issue as they are only poorly eliminated through conventional wastewater treatment. Advanced oxidation processes (AOPs), which have recently emerged as treatment technologies, aim to remove persistent pollutants. In the present work, the removal of anti-cancer drugs by photocatalytic membrane reactor is studied and compared with photolysis and peroxide treatments. 4 drugs were investigated: 5-Fluorouracil, Capecitabine, Cyclophosphamide and Ifosfamide. The study was conducted through kinetics-based, energy-based and economic assessment. Effects of the matrix (wastewater - laboratory grade water) and the presence of catalyst were first studied under irradiation of 2 low pressure (LP) mercury lamps. The addition of 1.5 $\left[\frac{g}{L}\right]$ of TiO_2 led to an improvement of the kinetics in both laboratory grade water and wastewater, while the passage from laboratory grade water to wastewater led to lower efficiency of both direct photolysis and photocatalysis. Agglomeration of TiO_2 in wastewater was also observed in comparison to laboratory grade water. Photolysis and photocatalysis experiments were then performed with a medium pressure (MP) mercury lamp, to investigate the influence of irradiation source on the degradation kinetics. Photolysis showed higher degradation rates than photocatalysis under the irradiation of medium pressure lamps, while both showed improved kinetics in comparison to low pressure lamps based photolysis and photocatalysis. On the other hand, medium pressure lamp based processes were observed to achieve a much less energy efficient degradation than the low pressure lamp based processes. UV(low pressure lamp)/H_2O_2 experiments, with H_2O_2 concentration of 0.05 $\left[\frac{g}{L}\right]$, were then performed in wastewater. The combination of photocatalyst and hydrogen peroxide was concluded to be inefficient, as proposing lower degradation rates and higher energy demands than UV-photolysis with H_2O_2 alone. Finally, LP-H_2O_2 photolysis was shown to be more efficient than direct photolysis and photocatalysis on all three kinetic, energetic and economic aspects.

Acknowledgements

First of all, I would like to thank my master thesis promoter, Patricia Luis Alconero, without whom this thesis could not have been possible. Prof. Luis Alconero was always available whenever I ran into a trouble spot or had questions about my research.

Another major actor is Raphael Janssens, who provided me guidance all along the realisation of this master thesis. He helped me to express my creativity through the solving of the unexpected problems encountered. He consistently allowed this paper to be my own work, but steered me in the right direction whenever I needed it.

I also would like to thank the technician team, and more particularly Helene Dailly, who was always available when technical support was needed.

In addition, I would like to express my gratitude to Professors Denis Dochain and Iwona Cybulska for accepting to be assessors of this thesis.

Finally, I must express my very profound gratitude to my parents for providing me with unfailing support and continuous encouragement. This accomplishment would not have been possible without them. Thank you.

Contents

List of Figures

List of Tables

List of Abbreviations

AOP	Advanced Oxidation Process
PMR	Photocatalytic Membrane Reactor
LP	Low Pressure
MP	Medium Pressure
WW	WasteWater
LGW	Laboratory Grade Water
EP	Emerging Pollutant
WWTP	WasteWater treatment Plant
HRT	Hydraulic Retention Time
E_{EO}	Electrical Energy per Order
FU	5-Fluorouracil
CP	Cyclophosphamide
CAP	Capecitabine
IF	Ifosfamide

Introduction

The wastewater composition is the reflection of the society from which it comes. As the society is in constant evolution, it is thus without surprise that an evolution of the wastewater composition has also been noticed. The last decades have seen a fast expansion of the worldwide industrialisation and the significant increase of the use of all sort of chemicals, leading to the emergence of a whole new set of pollutants that need to be taken care of. Furthermore, the simultaneous improvement of detection methods has provided scientists with a way to witness the appearance of those potentially toxic new chemical compounds. According to Geissen et al. [29], 700 substances of those so-called Emerging Pollutants (EPs) have been categorised in 20 classes.

Antineoplastic drugs represent a non-negligible part of the pharmaceutical compounds found in municipal and hospital wastewater [59]. These are drugs largely used in oncological treatments to fight the propagation of cancerous cells. They are designed to kill, by various mechanisms, fast growing cells such as those found in cancer tumours. The problem resides in their lack of selectivity, causing cytotoxicity to normal cells. In 2012, an estimated
14.1 million new cases of cancer were reported worldwide, and these figures are expected to grow to 23.6 new cases per year by 2030 [74]. Antineoplastic drugs are administrated in the order of hundreds of tons per year worldwide, a number that is logically expected to grow proportionately to the number of cancer cases[10].

Anti-cancer drugs are extremely persistent, and very poorly eliminated by conventional wastewater treatment plants (WWTPs) [46]. In order to efficiently eliminate pharmaceuticals from aqueous environments, wastewater treatment technologies must be improved and adapted to its evolving components. Numerous alternative treatments have been developed these last years, one of the most promising field of development being the so-called Advanced Oxydation Processes (AOPs). These are based on the generation of highly reactive oxidants (e.g. hydroxyl radicals) which degrade most organic pollutants rapidly and non selectively [67].

One of the AOPs currently being investigated is Slurry Photocatalytic Membrane Reactor (slurry PMR) as wastewater treatment. This process permits to combine the efficiency of photocatalyst suspension with the separation properties of membrane to efficiently retain the catalyst particles in the system. In his work, Janssens et al. [38] presented this technology as an emerging promising technology for wastewater treatment. Nevertheless, the factors influencing the photocalatytic degradation are plentiful, while still too few studies assessing their impacts have been published.

This master thesis will be performed in the frame of Raphael Janssens' PhD. The purpose will be to study the photocatalytic degradation of antineoplastic compounds under varying operating conditions and to compare its efficiency with direct UV-photolysis and UV/H_2O_2-photolysis

treatments. This will be done by (i) studying the degradation kinetics under various conditions such as presence of catalyst, matrix composition (laboratory grade water - wastewater), type of irradiation source (low pressure (LP) and medium pressure (MP) mercury lamps) and presence of hydrogen peroxide, (ii) determining the rate of energy emitted by the LP UV lamp and the MP UV lamp, that is usable to degrade the drugs, (iii) calculating the amount of energy that needs to reach the drugs molecules in order to reduce their concentration by one order of magnitude and (iv) performing a primary economical evaluation of the most promising studied processes.

Chapter 1

Literature review

1.1 Antineoplastic compounds

Pharmaceutics were first detected in aquatic environments during the 1970s, leading to a growth of the attention paid to them [34]. Among pharmaceutical compounds, drugs used for cancer treatment (i.e. antineoplastic agents) which represent a non-negligible part of those compounds, are suspected to present specific risks for aquatic species which are initially non-targeted [44]. Their intended function is to stop the proliferation of cancerous cells or simply to eliminate the tumorous cells by direct or indirect interaction with the DNA. While their effects on the human metabolism are well documented, their actions on the ecosystems remain unclear and not sufficiently assessed [61]. The reason of those suspicions is that antineoplastic compounds are known to be genotoxic, mutagenic, teratogenic and fetotoxic. Some authors stated that all eukaryotes organisms might be affected by their toxicity [66].

Different kinds of antineostatic compounds can be distinguished according to their mechanism of action.For instance, cytotoxic drugs are designed to interact with DNA, causing morphological and metabolic modifications of the cell, and eventually its destruction [10]. A further distinction can be made between cytotoxic compounds acting directly on the DNA (referred as DNA-interactive agents) and those who interact indirectly with DNA (for instance by acting on its synthesis) [30]. Cytostatic drugs do not act on the DNA, but lead by various mechanisms to a decrease in cancerous cells proliferation. For instance, some cytostatic agents act as inhibitors to cell growth factors, while others recruit cytotoxic cells, such as macrophages and monocytes [10]. A synthetic classification of antineoplastic compounds has been proposed by Besse et al. [10]. A reviewed version of this table is displayed on table 1.1.

Antineoplastic compounds are delivered in the order of hundreds of tons per year worldwide, a number which is expected to continue growing as does the annual new cancer cases. For instance, according to the French Health Products Safety Agency for cytotoxic and cytostatic drugs [22] [23], the French consumption amounts have increased from 13 t to 17.5 t between 2004 and 2008. Of course, amounts and types of drugs consumed greatly differ between countries [45].

Class	Mechanism of action	Detailed mechanism
Cytotoxics which interact directly with DNA	Alkylating agents	Inhibition/alteration of transcription
	Platinium complexes	Inhibition of replication
	Intercalating agents	Breaking of single-stranded DNA
Cytotoxics which interact indirectly with DNA	Antimetabolites	Blocking of the enzyme activity which leads to disrupting of DNA synthesis
	Cytotoxic antibiotics	Disturbing of the DNA synthesis by intercalating between DNA base pairs
	Mitotic spindle inhibitor	Inhibition of mitotic spindle formation
	Topoisomerase inhibitors	Blocking religation of double stranded DNA breaks
Cytostatics	Protein kinase inhibitors	Interaction with protein kinase, which regulates many biological processes

Table 1.1: Antineoplastic compounds classification [10]

The following table (cfr. figure 1.1) displays the 20 most consumed anticancer drugs in France for years 2004 and 2008, as well as their predicted environmental concentrations (Pecs) according to Besse et al. [10].

Molecule	Type of molecule	Chemical class	Total amounts 2004 (kg)	Total amounts 2008 (kg)	Conservative PEC 2004 ($ng\,l^{-1}$)	Conservative PEC 2008 ($ng\,l^{-1}$)
Hydroxycarbamide	Cytotoxic	Other	5756.67	6838.63	131.43	156.13
Capecitabine	Cytotoxic	Antimetabolite	2620.99	5134.94	59.84	117.24
Fluorouracil	Cytotoxic	Antimetabolite	1690.24	1733.20	38.59	39.57
Imatinib	Cytostatic	Tk inhibitor	583.68	873.90	13.33	19.95
Bicalutamide	Endocrine	Antiandrogen	n.a.	863.00	n.a.	19.70
Flutamide	Endocrine	Antiandrogen	n.a.	521.00	n.a.	11.90
Gemcitabin	Cytotoxic	Antimetabolite	339.21	379.28	7.74	8.66
Tamoxifen	Endocrine	Antiestrogen	n.a.	377.00	n.a.	8.61
Cyclophosphamide	Cytotoxic	Alkylating agent	281.84	305.73	6.43	6.98
Estramustine	Cytotoxic	Other	388.38	287.62	8.87	6.57
Mitotane	Cytotoxic	Other	95.90	233.75	2.19	5.34
Exemestane	Endocrine	Antiaromatase	n.a.	182.00	n.a.	4.16
Nilutamide	Endocrine	Antiandrogen	n.a.	169.00	n.a.	3.86
Erlotinib	Cytostatic	Tk inhibitor	0.00	148.85	0.00	3.40
Cytarabine	Cytotoxic	Antimetabolite	117.41	133.59	2.68	3.05
Lapatinib	Cytostatic	Tk inhibitor	0.00	116.20	0.00	2.65
Ifosfamide	Cytotoxic	Alkylating agent	121.38	103.04	2.77	2.35
Mercaptopurine	Cytotoxic	Antimetabolite	102.04	94.84	2.33	2.17
Bevacizumab	Cytostatic	Monoclonal ab	0.00	87.12	0.00	1.99
Carboplatin	Cytotoxic	Platinum derivative	64.38	83.59	1.47	1.91

Figure 1.1: Predicted environmental concentrations (PECs) for anticancer drugs, based on their consumption in France for years 2004 and 2008 [10]

For what concerns the relative importance of different sources for the introduction of anticancer drugs in the environment, it isstrongly depends on countries and their drug administration standards. In general, households effluents remain the main source of their introduction in the environment. For instance, only 13.8 % of the antineoplastics drugs used in France are released in hospitals wastewater [45].

After their administration, a large part of the drugs and their metabolites is excreted and ends into effluents. In most cases, the percentage of parent molecules remaining unchanged after ingestion and excretion varies between 10 and 80 % [32] [16].

Most antineoplastic compounds are highly soluble (predicted $\log K_{ow}$ between -1 and 3) [64]. Also, according to Kummerer et al. [45], most (around 89 %) of the antineoplastic compounds are not readily biodegradable. Furthermore, approximately 30 % of the antineoplastics have been found to be persistent when dissolved in the water phase [45].

The fact that antineoplastic drugs are strongly persistent, low biodegradable, highly soluble compounds, allied to their extreme dilution in effluents, make them extremely difficult to eliminate trough conventional wastewater treatment processes. Halling-Sorensen et al. [31] reported the concentration of some antineoplastic compounds, detected in treated wastewater effluents: Cyclophosphamide (146 $[\frac{ng}{L}]$) , Methotrexate (6.25 $[\frac{ng}{L}]$), ifosfamide (24 $[\frac{ng}{L}]$) and Bleomycin (13 $[\frac{ng}{L}]$).

This, and the dangers that it represents, shows the necessity of the development of new wastewater treatment technologies, able to efficiently eliminate antineoplastic compounds. The so called Advanced Oxidation Processes (AOPs) constitute one of the numerous alternative treatments that have been developed the last years, and will be detailed in the next section.

1.2 Advance Oxidation Processes (AOPs)

Advanced Oxidation Processes (AOPs) aim to remove persistent pollutants not eliminated currently by conventional WWTP, to meet the increasingly strict requirements fixed by environmental regulations. They have been largely investigated during the last decades and even applied in some treatments of industrial wastewater effluents [25]. Although AOPs technologies have already been considerably improved and the field of research greatly developed, they remain relatively young technologies and need further researches and development to reach maturity.

AOPs constitute a family of similar technologies that are based on the generation of highly reactive, and consequently short-lived, hydroxyl radicals, permitting to degrade non-selectively a large number of organic pollutants [67]. Furthermore, they offer varied processes for $OH^{\bullet}$ production, allowing to comply to specific treatment requirements. According to numerous studies [58] [19] [3], H_2O_2 photolysis, Fenton oxidation, Ozonation and Photocatalysis are among the most promising fields for the development of AOPs technologies. Sarasidis et al. [67] also described them as "simple and easy to implement at large scale". Those four processes will be briefly introduced in the next paragraphs, but there exists many more AOPs technologies, including processes combining two or more AOPs.

H_2O_2 photolysis H_2O_2 photolysis refers to processes effected through irradiation of the pollutant solution, containing hydrogen peroxides, with UV-light of wavelength smaller than 280 [nm] [58]. The absorption of light by hydrogen peroxide particulates causes their homolitic cleavage, forming hydroxyl radicals (cfr. eq. 1.1).

$$H_2O_2 \xrightarrow{hv} 2\,OH^{\bullet} \tag{1.1}$$

The formed hydroxyl radicals can then propagate through the following reactions:

$$OH^{\bullet} + \ + H_2O_2 \longrightarrow HO_2{}^{\bullet} + H_2O \tag{1.2}$$

$$H_2O_2 + HO_2{}^{\bullet} \longrightarrow H_2O + OH^{\bullet} + O_2 \tag{1.3}$$

According to Andreozzi et al. [3], the main drawbacks of the H_2O_2 photolysis is the small molar extinction coefficient of H_2O_2 (18.6 $\left[\frac{L}{mol\ cm}\right]$ at 254 [nm]), meaning that only a small fraction of the incident light is exploited. Kinetics of peroxide-based photolysis has been found to be improved at alkaline pH conditions, due to higher molar extinction of $HO_2{}^{-}$ species (240 $\left[\frac{L}{mol\ cm}\right]$ at 254 [nm]), which are in acid-base equilibrium with H_2O_2 [47]. The implied hydroxyl radicals generation mechanism is the following:

$$H_2O_2 \longleftrightarrow HO_2{}^{-} + H^{+} \tag{1.4}$$

$$HO_2{}^{-} \xrightarrow{hv} OH^{\bullet} + O^{-} \tag{1.5}$$

Due to its low molar adsorption, about 75 to 90 % of the influent H_2O_2 remains after UV

photolysis [40]. As hydrogen peroxide can cause toxicity through multiple mechanism, its use for disinfection treatments is generally followed by a quenching step to ensure hydroxyl radicals deactivation and elimination of the hydrogen peroxide molecules [76]. One of the used method for hydrogen peroxides quenching, which has shown to be efficient and inexpensive, is the addition of catalase in the reactor vessel. According to Liu et al. [50], a 0.2 $[\frac{mg}{L}]$ catalase dose is able to quench 100 [ppm] of H_2O_2 in less than 10 minutes.

Fenton Oxydation The Fenton Oxydation is based on the decomposition of hydrogen peroxides through reaction with iron ions, which leads to the formation of hydroxyl radicals. The main reaction, known as the Fenton reaction, is the following:

$$Fe^{2+} + H_2O_2 \longrightarrow Fe^{3+} + HO^- + OH^\bullet \tag{1.6}$$

The formed radicals can then oxidise organic compounds (RH or R) by hydrogen abstraction or hydroxyl addition, leading to the formation of $R^\bullet$ and $RH^\bullet$, highly reactive molecules that can be further oxidised. Furthermore, ferric ions Fe^{3+} formed through the Fenton reaction (cfr. eq. 1.6) can also react with H_2O_2, regenerating the $Fe_2{}^+$ ions and forming $HO_2{}^\bullet$ radicals. This reaction, known as the Fenton-like reaction is displayed in equation 1.7. Although $HO_2{}^\bullet$ species are less sensitive than $OH^\bullet$ radicals, they are still able to degrade organic compounds.

$$Fe^{3+} + H_2O_2 \longrightarrow Fe^{2+} + H^+ + HO_2{}^\bullet \tag{1.7}$$

Fenton and Fenton-like processes are little influenced by pressure and temperature conditions. They can then be carried out under atmospheric pressure and at room temperature. However, pH conditions strongly influence the efficiency of the reactions. This is due to the presence of Fe^{2+} and Fe^{3+} ions as well as to the speciation of H_2O_2. Studies have demonstrated that the optimum pH value allowing the Fenton reaction to occur is around 3, and that slight variations of the pH strongly decrease the efficiency of the process [52]. This is why hydrogen peroxide treatment rarely implies Fenton oxidation, as it would require a correction of the hydrogen peroxide pH which is typically between 7 and 8.

An alternative to the Fenton process, referred as photo-Fenton, takes advantage of UV-Vis ($\lambda > 300$ nm) light irradiation to facilitate the degradation of organic pollutants. In this particular case, Fe^{3+} complexes are photolysed, permitting the regeneration of the Fe^{2+} species. The photo-Fenton process implies equations 1.8, 1.9 and 1.10:

$$Fe^{2+} + H_2O_2 \longrightarrow Fe^{3+} + HO^- + OH^\bullet \tag{1.8}$$

$$Fe(OH)^{2+} \xrightarrow{hv} Fe^{2+} + OH^\bullet \tag{1.9}$$

$$H_2O_2 \xrightarrow{hv} 2\,OH^\bullet \tag{1.10}$$

Unfortunately, as for the Fenton process, the photo-Fenton process strongly depends on the pH conditions, which needs to stay around 2.8 [3].

Ozonation Ozonation-based AOPs refer to processes based on the use of ozone as oxidant for pollutant degradation. Degradation can occur following two different pathways: the first one consists in direct reaction of the organic pollutants with O_3, while the second consists in indirect reaction with $OH^{\bullet}$, generated by O_3 decomposition. The second pathway is favoured at high pH (> 6) [19], higher concentrations of hydroxyl ions leading to better decomposition of O_3 into hydroxyl radicals through a complex chain mechanism [62]. As hydroxyl radicals react much faster than ozone (reaction rates 10^6 to 10^9 times faster [58]), the degradation of the organic compounds are often more efficient at high pH. The process can also be enhanced by addition of hydrogen peroxides, as reaction of H_2O_2 with O_3 lead to the formation of $OH^{\bullet}$ and thereby allows to initiate the decomposition cycle of ozone [58].

Another way to improve the kinetics of the ozonation process would be through the use of heterogeneous or homogeneous catalyst. Numerous catalyst types have already been investigated, and among them an important number of metal oxides and metal ions. Although it sometimes led to significant acceleration of the reaction, in most cases however, the reaction mechanism remains unclear [58].

Photocatalysis The photocatalysis principle is based on the excitation of a semi-conductor material through absorption of high-energy photons, leading to the formation of holes (h^+) in the valance band and electrons (e^-) in the conduction band. The electrons and holes further react with oxygen and hydroxyl groups dissolved in water, producing highly reactive oxygen species, such as $OH^{\bullet}$ and $O_2^{\bullet -}$ [78]. Various semiconductor, such as TiO_2, ZnO, NiO and Cds, have been investigated to serve as photocatalysts [19].

The system studied by the present work for the elimination of antineoplastic compounds is a specific case of photocatalytic oxydation, namely the Slurry Photocatalytic Membrane Reactors (slurry PMRs). This process combines heterogeneous photocalysis and membrane technology, allowing an efficient elimination of the organic pollutants while retaining the catalyst particles in the system. This system, as well as the mechanism of photocatalysis and the factors influencing it, will be detailed in the next sections.

1.3 Photocatalytic Membrane Reactors (PMRs)

Photocatalytic membrane reactors are hybrid technologies which combine a photocatalytic reactor and a membrane filtration technology. The system is thus composed of two distinct parts with different purposes: a photocatalytic reactor used for the degradation of the pollutants and a membrane module used to confine the catalyst in the reactor. The first part consists of a feed line, a light source (generally in the UV wavelength range) and the catalyst. An aeration line procuring oxygen to the system may also be present. The degradation reactions of organic pollutants take place at the surface of the catalyst.

Several characteristics distinguish photocatalytic membrane reactors from conventional photoreactors: (i) retention of the catalyst in the reactor environment, (ii) continuous process with simultaneous separation of products and catalyst particles and (iii) possible control of the residence time in the reaction zone [55].

Two classes of PMRs are usually distinguished, the first one is characterized by the immobilisation of the catalyst on the surface of the membrane, while the second one is characterised by catalyst particles in suspension in the reactor. The first class allows high permeate quality and lower fouling tendencies [78], but present limited active surface as well as replacement of the membrane as unique way to regenerate the photocatalyst. The second class, called slurry PMR, needs a further step of filtration to retain and recover the catalyst particles but allows to overcome the two disadvantages of the first class and generally present higher photocatalytic efficiency [78]. To illustrate the general principle of PMR, the scheme of a slurry PMR is displayed on figure 1.2.

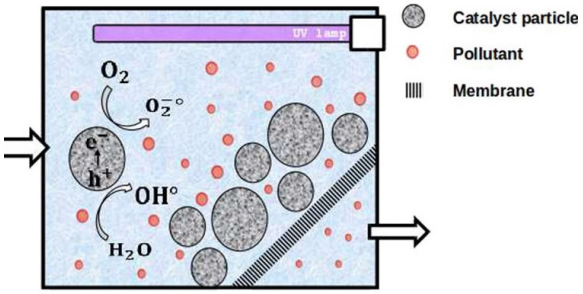

Figure 1.2: Principle of a slurry Photocatalytic Membrane Reactor [38]

The PMRs described in the literature generally use pressure membrane processes as membrane technology, such as microfiltration, ultrafitration and nanofiltration [55]. Those three processes are inevitably accompanied by the fouling of the membrane by the catalyst. New types of PMRs have recently been investigated, allowing to overcome this limitation: combination of photocatalysis with dialysis [7], pervaporation [12] and direct contact membrane distillation [57]. But further studies still need to be performed.

The present master thesis focuses only on the photoreactor part of a slurry PMR. No further development of the membrane technology part will be displayed in this work. This aspect has nevertheless been investigated by several authors [56] [38] [7]. The next section will thus focus on the precise mechanism of photocatalytic degradation in a slurry Photocatalytic Membrane Reactor and the different factors influencing its kinetics.

1.4 Photocatalytic degradation

1.4.1 General catalytic mechanism

To understand how photocatalysis works, it is important to have in mind the fundamentals of how a catalyst improves the kinetics of a reaction. A brief simplified reminder of what is a catalyst and how it works will be given in this section.

The Transition State Theory (TST) proposes a general explanation and a simple way to calculate the rates of elementary chemical reactions [6]. It assumes that reactant molecules, when meeting each other, form a transition state complex which is in "quasi-equilibrium" and shows maximum potential energy. In this activated complex, original liaisons of the reactants have weakened while new liaisons are only partially formed. Potential energy then decreases when rearranging the molecules to form the products (or to reform the reactants). In this way, only molecules disposing of sufficient energy can surpass this "energetic barrier" (i.e. activation energy) to form the products.

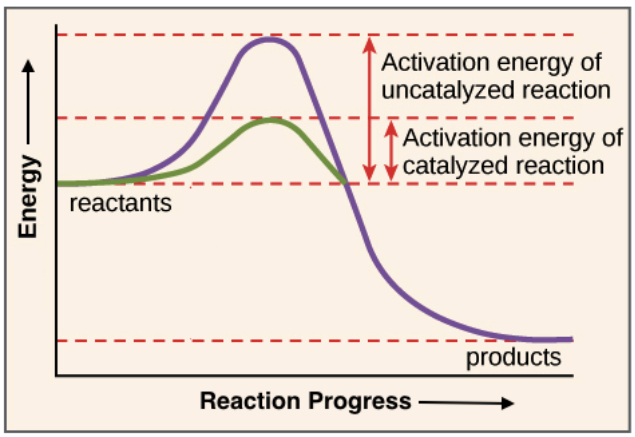

Figure 1.3: Reaction paths of a catalysed and uncatalalysed exothermic reaction [2]

The catalyst permits to decrease this activation energy by proposing an alternative reaction path (cfr. figure 1.3) which includes a transition state complex of lower potential energy [6]. A higher number of molecules are then able to pass the energetic barrier, improving the kinetics of the reaction. The degradation rate as a function of activation energy E_a is given by the Arrhenius law (cfr. equation 1.11):

$$k = A \exp\left(\frac{-E_a}{RT}\right) \tag{1.11}$$

Where k is the rate constant (in $\left[\frac{1}{s}\right]$ in the case of first order kinetics), E_a $\left[\frac{J}{mol}\right]$ is the activation energy, R is the Gas constant (8.314 $\left[\frac{J}{K\ mol}\right]$), T [K] is the temperature and A is the Arrhenius factor, indicating the rate of collision and the fraction of collisions with the proper orientation for the reaction to occur.

1.4.2 Mechanism of photocatalytic degradation

The excitation of a semiconductor particle takes place through irradiation of the material by a sufficiently energetic light beam. If the energy of the photons (hv) transported by the beam is higher or equal to the energy band gap (Eg) of the material, electrons (e^-) from the valance band (VB) are excited and promoted to the conduction band (CB) of the material, leaving positive holes (h^+) in the valance band. This results in the formation of e^-/h^+ pairs[54]. In the case of TiO_2, the generation of the e^-/h^+ pair is expressed as follow:

$$TiO_2 \xrightarrow{hv} TiO_2(e^- + h^+) \tag{1.12}$$

The generated holes and electrons can then either migrate to the surface of the semiconductor or recombine in the bulk with release of energy as heat or light. Electrons located at the surface are able to reduce organic compounds adsorbed on the surface, while holes located at the surface are able to oxidize them. For the photocatalytic process to be able to take place, both reduction and oxydation should be favoured thermodynamically, meaning that the redox potential of the species to be oxidised should be less positive than the valance band potential while the redox potential of the species to be reduced should be more positive than the conduction band potential0. [55]

The process consists in 4 main steps [55]:

1. Light absorption and (e-/h^+)pair formation;
2. Adsorption of the reactants at the surface of the semi-conductor;
3. Oxidation and reduction reactions;
4. Desorption of the generated products.

In the case of photocatalytic wastewater treatment, the oxidised species are surface hydroxyl groups or adsorbed water molecules. Hydroxyl radicals able to attack the compounds to be degraded are then formed:

$$OH^- + h^+ \longrightarrow OH^\bullet \tag{1.13}$$

$$H_2O + h^+ \longrightarrow H^+ + OH^\bullet \tag{1.14}$$

In parallel, dissolved Oxygen can be reduced into superoxide radicals anions:

$$O_2 + e^- \longrightarrow O_2{}^{\bullet -} \tag{1.15}$$

The formed superoxide radical anions $O_2{}^{\bullet -}$ can also produce hydroxyl radicals through a multistep reaction path that will not be detailed in this work. A detailed explanation of the mechanism has been presented by Molinari et al. [54]. A scheme of the main steps of the photocatalytic process is displayed on figure 1.4.

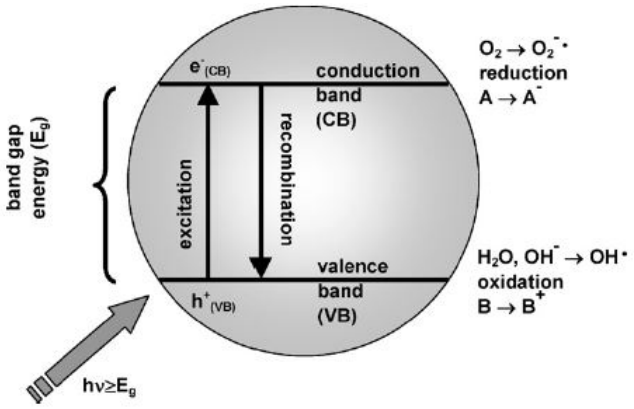

Figure 1.4: Schematisation of the photocatalytic process occurring at the surface of an activated semiconductor [55]

1.4.3 Photolysis

Photolysis can be defined as the chemical process by which chemical bonds are broken as a result of absorption of light energy by these bond [70]. This has been shown to cause the breakdown of many emerging contaminants [75]. When studying treatment technologies such as photocatalytic degradation of pharmaceuticals, it is thus important to keep in mind that direct photolysis may contribute to the degradation kinetics. The chemical equation of photolysis can simply be written as follows:

$$\mathrm{A} \xrightarrow{\mathrm{hv}} \mathrm{B} \tag{1.16}$$

Where A is the photolysed compound and B represents the photolysis products. The reaction rate for photolysis degradation of a specific compound mainly depends on the photo-chemical properties of the latter. The tendency of a compound to degrade under irradiation is characterised by its quantum yield for photolysis, i.e. the number of molecules decomposed by photon absorbed, and is dependant of the irradiation wavelength and intensity [75].

1.4.4 Degradation rates

Photocatalysis degradation rates of pollutants are generally described by a pseudo-first order rate constant (k) [38]. This corresponds to the slope of the linear regression presented in equation 1.17:

$$-\frac{d[C]}{dt} = k[C] \rightarrow \log\left(\frac{[C]}{[C_0]}\right) = k\ t \tag{1.17}$$

As degradation occurs, the pollutant concentration [C] decreases over time t. The use of the pseud-first order degradation constant k to compare performances of different processes is convenient since it is independent of initial concentration and time [38].

1.5 Factors influencing photocatalytic degradation

The basic principles of photocatalysis have been detailed in the previous section. In this section, the most important operating parameters affecting the degradation process will be described. They can be summarised as follows:

- Reactor design;
- Photocatalysts;
- Light source;
- Matrix composition;
- Temperature;
- Aeration and O_2 concentration.

1.5.1 Reactor design

As explained in section 1.3, photoreactors can be classified in two main groups depending on their design [55]: (1) fixed-bed photoactors and (2) slurry photoreactors. The configuration of interest in this work is the slurry photoreactor. The photocatalyst is evenly dispersed in the feed solution, while membrane technology is applied independently to recover the photocatalyst particles from the reaction solution [78]. The main advantages of this configuration is that photocatalyst and pollutant can interact through a larger surface area and do not suffer from mass transfer limitations through an immobilised catalyst layer. For those reasons, slurry photoreactor generally exhibits much higher degradation rates [78].

1.5.2 Photocatalysts

According to Mozia [55], a photocatalyst should exhibit the following characteristics: (i) high activity, (ii) poisoning resistance and stability during high pressure use, (iii) mechanical stability, (iv) low-selectivity and (v) physical and chemical stability. The ideal photocatalyst would also be low cost, available, activatable through visible light irradiation and would present high quantum yield. Due to their relatively low band gap, oxides and sulfides have largely been used as photocatalysts. The most common semiconductors used as photocatalysts according to Molinari et al. [54], as well as their band gap and activation wavelength (i.e. the minimum energy needed to activate the catalyst), are displayed on figure 1.5.

Photocatalyst	Band gap (eV)	Wavelength (nm)
SnO_2	3.8	318
TiO_2 anatase	3.2	387
TiO_2 rutile	3.0	380
WO_3	2.8	443
Fe_2O_3	2.2	560
ZnO	3.2	387–390
ZnS	3.7	335–336
CdS	2.5	496–497
CdSe	1.7	729–730
GaAs	1.4	886–887

Figure 1.5: Band gaps and activation wavelengths of the most common semiconductors used as photocatalysts [54]

Due to their energetically favourable band structure, their relatively high quantum yield, their low cost and high availability, TiO_2-based photocatalysts remain to this day, the most promising and most used photocatalysts. However, their wide band gap does not allow them to respond under visible-light [55]. As it has been underlined by Molinari et al. [54], this implies that their "potential as a green technology cannot be entirely fullfield". Recent studies have tried to find modifications techniques allowing to reduce the band gap of TiO_2 and consequently use it under visible light beam. In their article, Rehman et al. [60] made an overview of the different techniques capable to improve TiO_2 activity. Another lead that has been followed is the synthesis and test of lower band gap semiconductors that could be activated by the visible light spectrum [26].

According to Ardizzone et al. [4], the activity of titania strongly depends on its structural and morphological characteristics. TiO_2 can crystallise in three polymorphic forms: rutile and anatase, both showing tetragonal crystal systems, and brookite, showing an orthorombic crystal system. Among those three polymorphs, anatase is generally considered as the most efficient due to its low recombination rate of its photogenerated electrons and holes [4]. Some authors reported that mixing titania phases can lead to enhanced photocatalytic activity, due to decreased recombination of photogenerated electrons and holes [77] [31]. To this day, the internationally most used photocatalyst for environmental purposes is the P25-TiO_2, a catalytic powder composed of 70 % TiO_2-anatase and 30 % TiO_2-rutile [18]. Also, according to Ardizzone et al. [4], maximisation of the active surface and minimisation of the particulates size permits to optimise the catalytic efficiency.

1.5.3 Light source

1.5.3.1 Type of lamp

The choice of the irradiation source is of major importance when studying photocatalytic degradation. It can impact both photocatalytic activation and direct photolysis of target compounds [51]. As seen in section 1.5.2, rutile and anatase crystalline forms of TiO_2 need irradiation of wavelength smaller than 380 and 387 [nm] respectively (cfr. figure 1.5) to be activated. Irradiation in the UV light range ($\lambda \in$ 100-400 [nm]) is thus needed to perform

photocatalytic degradation. Conventional lamps such as mercury lamps have been widely used as irradiation source for photocatalytic degradation [20], but the number of publications reporting photocatalytic applications based on LED light sources is increasing each year [69].

UV Mercury vapour lamps UV light is generated through the application of a voltage across mercury vapour, resulting in a discharge of photons. The output of light depends on mercury concentration in the gas phase, and thus on mercury vapour pressure [24]. Low pressure lamps ($\simeq 1$ [Pa]) generate monochromatic light centred at 254 [nm] while medium pressure lamps ($\in [10 : 100]$ [kPa]) show much larger emission spectra, from 200 [nm] up to 800 [nm] depending on the lamp. The latter show significantly higher power input and operating temperature ($\in 600 - 900°C$) [24]. The broad spectrum of the MP lamps permits to efficiently remove many micropollutants by direct photolysis. For this reason, the contribution of photolysis to the overall degradation is generally higher for MP lamps than for LP lamps. On the other hand, LP lamp irradiation tends to more efficiently generate hydroxyl radicals than MP lamp irradiation. Also, if MP lamps propose high power output and density, their efficiency to transform electrical power input into UV light is generally much lower than for low pressure mercury lamps. [35]

UV-LEDs Light is generated through the application of a current on a semiconductor material. Electrons and holes are generated in the conduction and valence bands of the semiconductor, and release energy in the form of light when recombining. They offer many advantages over conventional mercury vapour lamps : higher efficiency to convert electricity to light, longer lifetime (up to 5 times that of mercury lamps), easily adaptable output ("tunable" wavelength) and instant on-off [51][69]. Furthermore, they permit to avoid the use of mercury, which is recognised to be toxic [51]. Some authors, however, evaluated the overall removal efficiency of LED-based processes to be lower that of mercury lamps-based processes [48][41].

1.5.3.2 Intensity

The photocatalytic reaction rate usually increases with light intensity, as long as the intensity does not become too high. Zheng et al. [78] divided the influence of light intensity on photocatalytic performance in three different stages:

1. Low light intensity: the formation reactions of e^-/h^+ pairs are predominant compared to their recombination. The reaction rate increases linearly with light intensity;

2. Middle light intensity: formation and recombination reactions compete with each other. The reaction rate increases proportionally to the square root of light intensity;

3. High light intensity: the reaction rate does not vary anymore with light intensity.

1.5.4 Matrix composition

It is well known that the performance of TiO_2 photocatalytic processes strongly depends on the water matrix quality. Indeed, the presence of many organic and inorganic compounds tend to affect, sometimes significantly, the photocatalytic degradation efficiency [68]. Sarasidis et al. [68] have studied photocatalytic oxydation of diclofenac in three different water qualities (ultrapur water, ground water and top water), and shown that the purer the water, the more efficient the mineralization can be (cfr. figure 1.6).

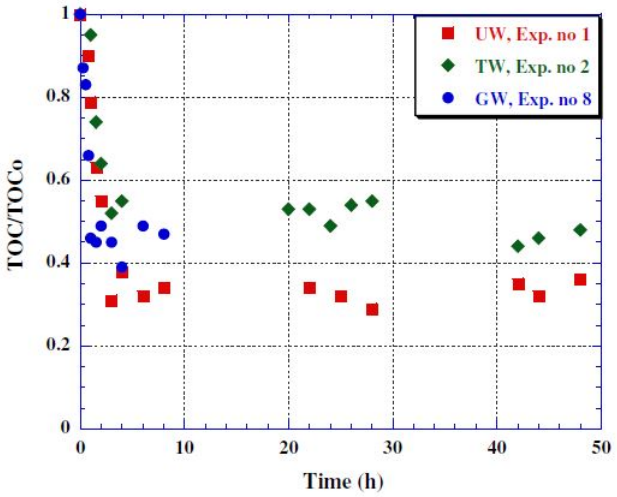

Figure 1.6: Sarasidis et al. [68] study of temporal variation of photocatalytic mineralization of DCF, expressed in terms of normalized TOC concentration, in the permeate stream, for different water types: ultrapure water (UW), ground water (GW) and top water (TW). $[TiO_2] = 0.75\ [\frac{g}{L}]$

A large number of constituents of wastewater might influence photocatalytic oxydation. Some of the most often cited in the literature are briefly introduced in the next sections.

1.5.4.1 Initial pollutant concentration

The initial pollutant concentration in a wastewater stream plays an important role on the treatment efficiency. Two different phenomenons compete with each other [78]: on the one hand, a higher pollutant concentration means higher probability of reaction between the targeted compounds and the oxidative species and thus results in higher degradation rate; on the other hand, a more concentrated solution becomes more opaque, reducing the light penetration length. Furthermore, pollutants at higher concentration are more likely to fix themselves to the active sites of the photocatalyst, leading to their deactivation.

In theory, degradation rate thus first improves with the increase of the pollutant concentration, but then decreases if the pollutant concentration is further increased [78]. However, in the case of antineoplastic compounds, which are extremely diluted in wastewater streams, opacity of the solution and catalyst deactivation are unlikely to be caused by antineoplastics concentration [31]. Non-targeted pollutants may, on the other hand, be at the origin of these phenomena.

1.5.4.2 Catalyst load

In most cases, increasing the initial catalyst load of the system permits to increase the active surface area, leading to an improvement of the degradation rate and efficiency. However, too high catalyst load would lead to an increase of the opacity of the solution, reducing the penetration of the photons in the solution [78]. Furthermore, agglomeration of the photocatalyst particles is more likely to happen at high catalyst concentration, leading to reduction of the active surface of the catalyst, and thus of the photocatalytic efficiency [49]. An optimum should then be observed, below which it is unnecessary to rise the catalyst load.

Other parameters, such as pH, presence of cations and organic matter content can influence the agglomeration of the catalyst particulates. According to Zheng et al. [78], agglomeration of TiO_2 particulates is enhanced at low pH. As wastewater effluents present neutral pH, which is conserved through the studied processes, no further discussion about the influence of the pH on photocatalytic degradation will be performed. The influence of the presence of cations and organic matter on the catalyst agglomeration will be discussed in the following sections.

1.5.4.3 Dissolved Organic Matter

The presence of organic matter may influence both direct photolysis and photocatalysis of target compounds by various mechanisms [14]: (1) reduction, by competitive scavenging, of the effective $OH^{\bullet}$ concentration available to react with the pharmaceuticals, (2) competitive adsorption on catalyst particulates, and (3) absorption of incident photons, reducing their availability for TiO_2 excitation.

Also, the presence of natural organic matter in matrix can induce bridging effects between TiO_2 particulates, which, according to Topuz et al. [73], is one of the main mechanisms leading to agglomeration of catalyst particulates in wastewater matrices.

1.5.4.4 Inorganic ions

Specific ions present in wastewater matrices may partially deactivate the TiO_2 particulates [68]. Indeed, relatively positively charged catalyst particulates can adsorb negatively charged contaminants, while negatively charged catalyst particulates can adsorb positively charged contaminants, forming a layer of charged barrier [55]. This can hinder the interaction between the target compounds and the surface of the catalyst. For instance, the isoelectric point of P25 Degussa catalyst being at pH 6.8, and wastewater pH being typically between 7 and 8, it is likely to be deactivated under the presence of positively charged inorganic ions in water matrices. Also, according to Topuz et al. [73], the presence of divalent cations screening the surface of the catalyst may induce a reduction of the energy barrier for stability of the TiO_2 particulates, leading to increased agglomeration of the catalyst.

1.5.5 Temperature

It is widely acknowledged that the variation with temperature of a chemical reaction follows the Arrhenius law that was introduced in section 1.4.1:

$$k = A \exp\left(\frac{-E_a}{RT}\right) \tag{1.18}$$

If the temperature increases, the temperature factor increases, which reduces the negative exponential term and subsequently increases the reaction rate [8]. However, as photocatalytic reactions are caused by photonic activaion (i.e. induced by light absorption), the true activation energy is nil and the apparent activation energy is negligible in the medium range of temperature [17]. Numerous authors [55] [78] have found that, between 20^oC and 80^oC, the efficiency of the photocatalytic degradation is barely affected by the variation of temperature. Temperature must be raised above 80 ^oC for the first non-negligible effects on the process to be observed. At this temperature, recombination of the charge carriers are favoured, which decreases the efficiency of the photocatalytic process and increases the apparent activation energy [33]. At very low temperature (below 0°C) the desorption of the products becomes the limiting step, as the apparent activation energy is increased and thus the efficiency of the process decreases.

1.5.6 Aeration and O_2 concentration

The aeration of the system increases the concentration of dissolved oxygen in the solution. As can be seen in section 1.4, dissolved oxygen plays an important role in the photocatalysis process, since it is implied in the production of hydroxyl radicals, and acts as electron scavengers to prevent recombination of the electrons present in the valance band. Furthermore, aeration in the case of suspended catalyst particles can help to keep a good dispersion of the photocatalyst in the reactor and at the same time facilitate the contact between target compounds and catalyst particles [78]. However, Chin et al. [21] observed that too high aeration rates lead to bubble clouds formation impacting the transmission of light in the solution.

Chapter 2

Objectives and research questions

At this stage of the report, the concerns about antineoplastic drugs and their delivery into the environment have been described, as well as the different treatment technologies that that can be used to eliminate them from wastewater effluents. This was necessary in order to define the objectives of this master thesis and the means that will be put in place to achieve them.

The main objective is to study the photocatalytic degradation of antineoplastic compounds under varying operating conditions and to compare its efficiency with direct UV-photolysis and UV/H_2O_2-photolysis treatments. This study is based on a triple approach : (i) degradation kinetics, (ii) energy consumption and (iii) costs assessment.

Kinetics based approach

The kinetics based approach is the core of the research and will serve as base for the energy consumption and economic assessment. It is to be realised through the answer of the following research question:

- What are the effects of the parameters listed below on antineoplastics degradation kinetics?
  - Presence of catalyst (TiO_2);
  - Laboratory Grade Water (LGW) matrix, wastewater (WW) matrix;
  - LP, MP lamp;
  - Presence of hydrogen peroxide (H_2O_2).

The method used to answer this question is a so-called Cytostatics Degradation Experiment with varying operating conditions that will be detailed in the Materials and Methods section (cfr. section 3.2.1).

Energy based approach

The energy consumption assessment goes through the answer of two distinct related questions:

- What is the rate of energy, emitted by the low pressure (LP) UV lamp and the medium pressure (MP) UV lamp, that is usable to degrade the drugs ?
- What is the amount of energy that needs to reach the drugs molecules in order to reduce their concentration by one order of magnitude ?

The answer of those two research questions will be procured through the calculations of the so-called Fluence rate and Electrical Energy per Order (EEO), two methods that will be detailed in the Material and Methods section (cfr. section 3.3).

Economic approach

The economic approach aims to procure a preliminary economic evaluation of pre-selected processes and operating conditions. This pre-selection will be realised through the discussion of the results of the two first approaches. The hypotheses and limits of the system considered for the costs assessment will be detailed in the Material and Methods section (cfr. section 3.4).

The aim is to answer the following question:

- Among the studied processes and operating conditions, what are the most advantageous ones on an economic point of view ?

Chapter 3

Material and methods

3.1 Set-up of the installation

The set-up consisted in an emerged annular batch photoreactor of 1.3 L, covered in aluminium foil to prevent outside irradiation to enter the reactor vessel. The reactor contained one UV lamp, centrally-located, or two UV lamps, symmetrically placed, depending on the experiment. In both cases, the lamps were placed in transparent quartz sleeves to prevent abrasion.

Homogeneous mixing of the solution was ensured by a magnetic stirrer with a stirring rate set at 500 rpm. A LAUDA MICROCOOL MC250 cooling system, connected to the reactor vessel, ensured a stable temperature of 20 $\pm 1^{o}$C during all the experiments. A temperature probe was used to monitor the deviations of the temperature.

A scheme of the set-up is displayed on figure 3.1.

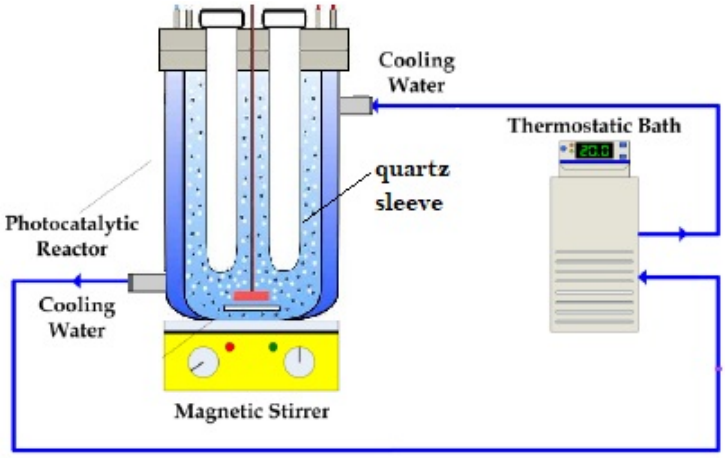

Figure 3.1: Schematic representation of the used set-up. Scheme modified from Sarasidis et al. [67]

Two different types of UV lamps were used during the experiments, low pressure (LP) UV-C germicide lamp (10 W) with a monochromatic spectra concentrated around 254 nm, and a medium pressure (MP) UV-A lamp (125 W) with a broader spectra in the UV region, both supplied by Helios Quartz. The emission spectrum of the latter is displayed on figure 3.2.

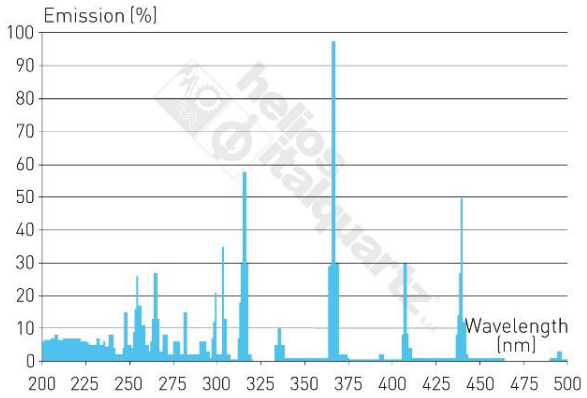

Figure 3.2: Emission spectrum of the used MP lamp, provided by the supplier

Sampling was done using disposable syringes, which were rinsed three times with 6 mL of mQ water between each sample. For the experiments using solutions of wastewater and/or solutions containing catalyst, PES filters with pore size 0.2 [μm], provided by VWR international, were used to prevent catalyst and other particles to get into the sampling vials. The cleaning of the filters was assured by passing 6 mL of mQ water through it.

3.2 Kinetics based approach

3.2.1 Cytotoxics Degradation Experiment

The Cytotoxics Degradation Experiment consisted in a series of experiments with varying operating conditions but the same methodology. The aim was to study the effect of the following operating conditions on the degradation kinetics of the drugs:

- Catalyst - TiO_2;
- Matrix - LGW or WW;
- Irradiation - LP or MP lamps;
- Peroxide - H_2O_2.

Specific materials

Part of the experiments were conducted using Laboratory Grade Water (LGW), the others were conducted using biologically treated sewage effluents provided by the wastewater treatment plant of Louvain-la-Neuve. The latter will be referred as wastewater (WW) in the rest of this report. The specifications of the wastewater, provided by the supplier, are presented in table 3.1 :

Compound	DBO	DCO	MES	NKj	N-NH_4	N-NO_3	N tot	P tot	P-PO_4	Cl
C $[\frac{mg}{L}]$	0.5	10.7	0	2.42	0.23	2.97	5.42	3.2	3.15	510

Table 3.1: wastewater specifications - wastewater treatment plant of Louvain-la-Neuve

The wastewater was stored in the dark at 4°C, and tested within 10 days after the sampling.

Four different drugs were selected among the 20 most consumed anticancer drugs in France for years 2004 and 2008 according to Besse et al. [10]. They are presented in figure 1.1. These four anticancer drugs, provided by Sigma-Aldrich, are presented in table 3.2.

Name	**Abreviation**	**Empirical formula**
5-Fluorouracil	FU	$C_4H_3FN_2O_2$
Cyclophosphamide	CP	$C_7H_{15}Cl_2N_2O_2P \cdot H_2O$
Capecitabine	CAP	$C_{15}H_{22}FN_3O_6$
Ifosfamide	IF	$C_7H_{15}Cl_2N_2O_2P$

Table 3.2: Used cytotoxics provided by Sigma-Aldrich

The abbreviations introduced in table 3.2 will be used frequently in the rest of this document. Stock solutions of 1 $[\frac{g}{L}]$ were prepared diluting the pharmaceuticals in a solution of mQ water which was stored in the dark at -20°C. For each experiment, the drugs were spiked at 500 ppb, which represented a high enough concentration to observe the degradation, as LoQ (limit of Quantification using analysis methods) of the drugs were determined to be of 10 ppb by the technician of the research team.

TiO_2 was selected to be used as photocatalyst, given the fact that it is still, to this date, the most used photocatalyst in the industry [55]. A catalytic powder mixture, of 70 % TiO_2-anatase

and 30 % TiO_2-rutile (P25-TiO_2) was supplied by Degussa (Germany) and stored in the dark at room temperature to avoid unwanted activation.

A fixed catalytic load of 1.5 $[\frac{g}{L}]$ was selected for all experiments conducted in presence of TiO_2, based on previous researches performed by Raphael Janssens' research team about catalyst load optimisation in pure water. For this study, pCBA molecular probe and a LP lamp with monochromatic emission spectrum concentrated at 255 nm were used. It can be seen on figure 3.3 that the degradation rate reached a plateau at 1.5 $[\frac{g}{L}]$, a concentration of catalyst thus useless to exceed.

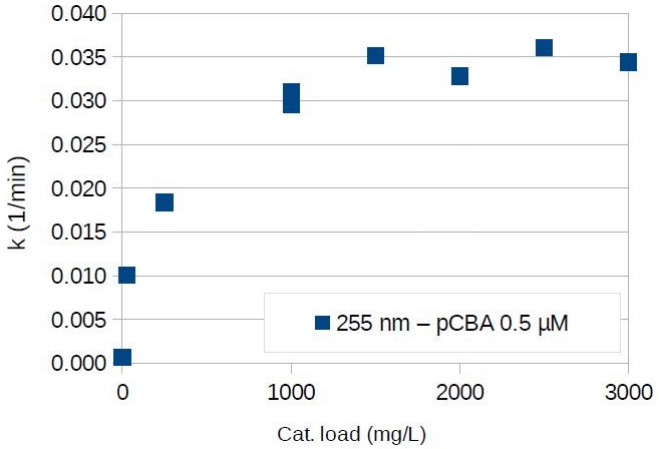

Figure 3.3: Catalyst load optimisation performed by Raphael Janssens' team using pCBA and LP lamps of 255 nm

The peroxide was supplied by Sigma-Aldrich and stored in the dark at -20°C. A fixed peroxide load of 50 [ppm] was selected for all experiments conducted in presence of H_2O_2, based on an optimisation performed by Miralles-Cuevas et al. [53] on a 100 L pilot plant.

Methodology

A scheme of the methodology is displayed on figure 3.4.

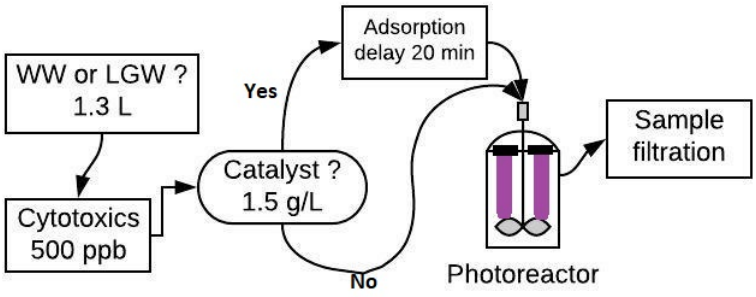

Figure 3.4: Scheme of the Cytotoxics Degredation Experiment

The first step was the positioning of the LP or MP lamps. For the experiments using MP lamps, only one lamp was used, and had to be switched on 30 minutes before the start of the experiment in order to be fully operational. In this case, the solution was prepared in a flask outside of the reactor vessel, mixed regularly and stored in the dark until the start of the

experiment. In the case of experiments with LP lamps, two lamps were used, and the reaction solution was directly prepared in the reactor vessel as no delay is needed in order for the LP lamp to be operational. The lamps were switched on directly at the start of the experiment.

The second step was the preparation of 1.4 L of the reaction solution; 1.3 L to be used for the degradation reaction and 0.1 L used for control tests. The drugs were spiked in 1L of the medium - WW or LGW - before the addition of the 0.4 L left, together with the catalyst powder if needed. In this case, a delay of 20 minutes was respected between the addition of the catalyst and the beginning of the experiment. This was done to reach the adsorption equilibrium of the drugs on the catalyst particles.

For the experiments realised in presence of peroxide, it was added in the reaction solution just before the start of the experiment, to prevent premature degradation as peroxides are very reactive species.

A summary of the realised cytotoxics degradation experiments is displayed in table 3.3.

N°	**Name**	**Lamp**	**Medium**	**TiO_2 $[\frac{g}{L}]$**	**H_2O_2 [ppm]**
1	LGW - LP	2 LP	LGW	0	0
2	LGW - LP/TiO_2	2 LP	LGW	1.5	0
3	WW - LP	2 LP	WW	0	0
4	WW - LP/TiO_2	2 LP	WW	1.5	0
5	WW - MP	1 MP	WW	0	0
6	WW - MP/TiO_2	1 MP	WW	1.5	0
7	WW - LP/H_2O_2	2 LP	WW	0	50
8	WW - LP/H_2O_2/TiO_2	2 LP	WW	1.5	50

Table 3.3: Summary of Cytotoxics Degredation experiments

To refer to the different experiments, the names presented in table 3.3 will be used frequently below.

For each experiment, samples (1-1.5 mL) were taken at times 0 - 3 - 6 - 12 - 20 - 30 [min]. Control samples (1-1.5 mL) were taken at times 15 - 32 [min]. For the degradation underwent in WW medium, Samples of 5 mL were taken just before and after the experiments and sent to DOC analysis, to study the decrease of the content in organic matters.

3.3 Energy based approach

3.3.1 Atrazine actinometry

Actinometry is a simple and accurate method used frequently for radiation measurement. It permits the calculation of the so-called Fluence rate, which can be defined as "the total radiant power, incident from all directions onto a small sphere divided by the cross-sectional area of that sphere" [36]. In other words, and in our specific case, it permits to calculate the amount of energy that is sent to the reactor volume, through the interface area between the lamp and the solution.

A chemical actinometer is a substance in which photochemical conversion is directly proportional to the number of photons absorbed. By studying its degradation kinetics, and knowing this specific relation between photochemical conversion and the absorbed energy, it is thus possible to calculate the amount of energy that gets to the actinometer per unit of time, and thus the radiant power that is sent to the reactor vessel.

According to the IUPAC Technical Report about chemical actinometry [42], the UV fluence rate, denoted as I $\left[\frac{Einstein}{s\ L}\right]$, can be calculated following equation 3.1:

$$I = \frac{\Delta A_\lambda}{\epsilon_\lambda\ l\ \Phi_\lambda\ t}\left[\frac{Einstein}{s\ L}\right] \tag{3.1}$$

Using the Lambert-Beer law, equation 3.1 can be rewritten as equation 3.2:

$$I = \frac{\Delta C\ \epsilon_\lambda\ l}{\epsilon_\lambda\ l\ \Phi_\lambda\ t} = \frac{\Delta C}{\Phi_\lambda\ t} = C_0\frac{\exp kt - 1}{\Phi_\lambda\ t}\left[\frac{Einstein}{s\ L}\right] \tag{3.2}$$

Where A is the absorbance at wavelength $\lambda[nm]$, l $[cm]$ the optical pathlength, ϵ $\left[\frac{L}{mol\ cm}\right]$ the molar adsorption coefficient, t [s] the irradiation time, k $\left[\frac{1}{s}\right]$ the pseudo first order degradation constant of the actinometer and Φ_λ $\left[\frac{mol}{Einstein}\right]$ the quantum yield of the actinometer. This latter is specific to each actinometer, and defined by the IUPAC Technical Report about chemical actinometry [42] as "the number of events, e.g., molecules changed, formed, or destroyed, divided by the number of absorbed photons of that particular wavelength in the same period of time." When studying the UV fluence of a lamp, the quantum yield of an actinometer needs to be known for the entire emission wavelengths range of the lamp for the actinometer to be usable to characterise this lamp.

Atrazine is a widely used actinometer, as the value of its quantum yield at $\lambda = 254$ [nm] has been studied and is known to be equal to 0.05 $\left[\frac{mol}{Einstein}\right]$ [9]. That makes it suitable for the characterisation of lamps with emission spectra centred at 254 nm. According to Rosenfeldt et al [63], this value can also be used as good approximation of the average quantum yield of atrazine in the wavelength range of 200-300 nm. That makes atrazine suitable to estimate the UV Fluence rate of lamps with broader emission spectra.

Knowing that 1 Einstein = $\frac{0.119627}{\lambda}$, equation 3.2 can be rewritten as follow:

$$I = C_0\ \frac{(\exp kt - 1)}{t}\ \frac{0.119627}{0.05\ \lambda}\left[\frac{J}{s\ L}\right] \tag{3.3}$$

The used LP lamp having a monochromatic emission spectrum of 254 nm, the calculations of

its UV Fluence can be rewritten as:

$$I = C_0 \ \frac{(\exp kt - 1)}{t} \ \frac{0.119627}{0.05 \ 254} \left[\frac{J}{s \ L}\right] \tag{3.4}$$

For what concerns the MP lamps, equation 3.3 can be integrated on the wavelength range of 200-300 nm, giving equation 3.5:

$$I = C_0 \ \frac{(\exp kt - 1)}{t} \ \frac{0.119627 \ \log\left(\frac{3}{2}\right)}{0.05} \left[\frac{J}{s \ L}\right] \tag{3.5}$$

k, the pseudo first order degradation rate of atrazine under the action of the lamps and t [s], the irradiation time, are to be determined experimentally.

Fluence rates were calculated for 1 LP lamp, 2 LP lamps and 1 MP lamp.

Experimental methodology

The experimental part aimed to study the degradation kinetics of atrazine under the action of the different lamps and the calculation of the pseudo first order degradation constants to be used in equations 3.4 and 3.5. Atrazine was supplied as a powder by Sigma-Aldrich. Stock solutions of 1 $\left[\frac{g}{L}\right]$ were prepared diluting the atrazine powder in a solution of mQ water which was stored in the dark at -20°C.

It consisted in the photolysis of 1.3 L of a solution of atrazine spiked at a concentration of 10 ppm in LGW. The selection of the atrazine concentration to be degraded was based on a preliminary determination of the calibration curb of the compound. A scheme of the experimental method is represented on figure 3.5.

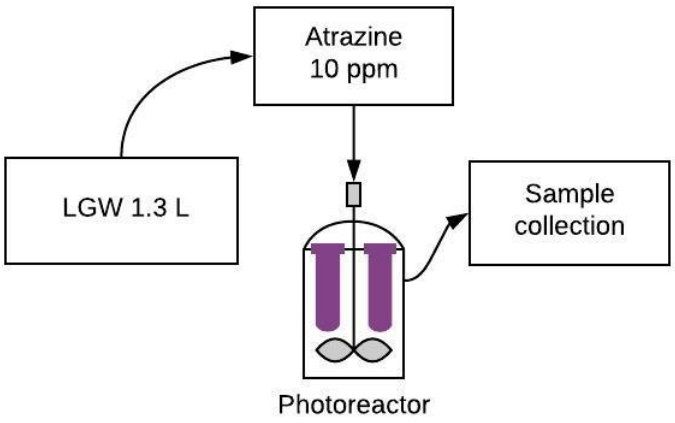

Figure 3.5: Experimental method for the determination of degradation rates of atrazine

For the characterisation of the MP lamp, two experiments were realised, to ensure the reproducibility of the experimental method. Samples were taken at times 0 - 2 - 4 - 6 - 10 - 15 [min] during the first experiment. As all the atrazine was degraded in less than 10 [min], the second experiment was realised in 8 [min], with sample collection at times 0 - 1 - 2 - 4 - 6 - 8 [min]. The two last experiments were realised under the action LP lamps (one lamp during the first one and two lamps in the second one) and samples were collected at time 0 - 5 - 10 - 15 - 20 - 30 [min].

3.3.2 Fluence-based EEO Calculation

The energy efficiency of UV based AOPs is usually quoted in terms of Electrical Energy per Order [5]. It can be defined as the number of kilowatt hours of electrical energy required to reduce the concentration of a contaminant by one order of magnitude (90% removal) in one m^3 of water [11]. For a batch operation, it is generally calculated as in equation 3.6:

$$E_{EO} = \frac{1000\ P\ t}{V\ \log \frac{C_0}{C_f}} \left[\frac{kWh}{m^3\ order}\right] \tag{3.6}$$

Where P is the rated power [kW] of the system, V is the volume [L] of water treated in the time t [h], C_0 and C_f the initial and final concentration of the pollutant [M]. The particularity of this work is that the E_{EO} calculation was not based on the rated power of the system, but on the amount of energy that is actually sent to the reactor i.e. the UV Fluence rate. Equation 3.6 can thus be rewritten as follow:

$$E_{EO} = \frac{1000\ I\ t}{V\ \log \frac{C_0}{C_f}} \left[\frac{kWh}{m^3\ order}\right] \tag{3.7}$$

Where I is the UV Fluence rate, given in [kW]. In the case of pseudo first-order kinetics, it can be written :

$$\log \frac{C}{C_0} = k_{obs}\ t \tag{3.8}$$

Equation 3.7 becomes equation 3.9:

$$E_{EO} = \frac{1000\ I}{V\ k_{obs}} \left[\frac{kWh}{m^3\ order}\right] \tag{3.9}$$

Where k_{obs} isthe pseudo first-order kinetics constant $\left[\frac{1}{h}\right]$.

The Fluence rate based E_{EO} was calculated for all the studied processes and operating conditions, but with the specific aim to be able to compare processes using different UV lamps.

3.4 Economic approach

3.4.1 Preliminary economic evaluation

When it comes to the adoption of a treatment process at the industrial scale, favourable process economics are of the highest importance. If a precise economic evaluation is complicated to achieve through pilot scale experimentation, it is nevertheless possible to attempt a preliminary economic evaluation. What is important is to clearly define the limits of this preliminary study, as well as the hypotheses on which it is based.

An estimation of the operating costs of the two most promising studied processes, selected through the kinetics and energy based approaches, was performed based on the experiments carried out in the pilot-scale reactor.

The prime hypothesis is the treatment of 1 m^3 of wastewater, operated in the pilot-scale batch reactor of 1.3 L, and leading to the decrease of the pollutants concentration by one order of magnitude. The system was limited to the acquisition of the different reactants, the replacement of the lamps and membranes and the supply of energy to the lamps and pumps for the duration of the treatment. The costs related to investment, labour, maintenance and transport were not taken into account.

Degradation through TiO_2-based process was supposed to be coupled to a filtration step using a membrane technology. Degradation through H_2O_2-based process was supposed to be coupled to a H_2O_2 deactivation step by the action of catalase (cfr. section 1.2).

The duration of the treatment, that will be denoted as HRT (hydraulic retention time), was calculated as the time needed to decrease the concentration of the slower-degrading drug by one order of magnitude through the studied process:

$$HRT = \frac{-\log(10)}{k}[min] \tag{3.10}$$

Where k $\left[\frac{1}{min}\right]$ is the pseudo first-order degradation constant of the slower degrading drug by the mean of the two studied processes.

Since the lamps, membrane and catalyst are only used for a duration corresponding to the HRT, the cost of their use was estimated based on the $\frac{HRT}{life\ time}$ ratio and their buying price. All the buying prices of the reactants, as well as the price of energy, have been considered to be fixed.

3.5 Analytical methods

3.5.1 HPLC-MS

Antineoplastic compounds analysis and quantification were performed through Hight Performance Liquid Chromatrography coupled with Mass Spectrometry (HPLC/MS).

HPLC/MS analyses were performed through an Agilent 6100 series single quadrupole LC/MS apparatus. The LC apparatus works extracting 5 µL from the sample vial at a speed of 8 $\left[\frac{\mu L}{s}\right]$, using a mechanical syringe. Each sample volume is then pumped at 10 bars and sent through an elution column (HSS5 column). The temperature of the column is kept at 30°C, and the mobile phase flowrate set to 250 $\left[\frac{\mu L}{min}\right]$.

The mobile phase was obtained by mixing two different solvents: solvent A (5% CH_3CN in water) and solvent B (100% CH_3CN). The elution of the antineoplastic compounds was eased by the variation of composition of the mobile phase, as can be seen in table 3.4.

Time [min]	% of A	% of B
0	100	0
3	100	0
9	65	35
12.5	65	35
15	50	50
17.5	5	5
20	5	5
22	100	0
25	100	0

Table 3.4: Mobile phase composition

Mass-to-charge ratios $(\frac{m}{z})$ used by the mass spectrometer to detect the cytotoxic compounds are reported in table 3.5.

compound	$\frac{m}{z}$ **ratio**	**mode**
5-Fluorouracil	129	negative
Cyclophosphamide	261	positive
Capcitabine	360	positive
Ifosfamide	261	positive

Table 3.5: $\frac{m}{z}$ ratios of the studied compounds

3.5.2 HPLC-UV

Atrazine analysis and quantification was performed through High Performance Liquid Chromatrography coupled with UV detection (HPLC/UV). The used apparatus was an Agilent 1200 series diode array and multiple wavelength detector SL.

The LC apparatus is quite similar to the one of the HLPC-MS explained earlier, 5 μL are extracted from the sample vial, then sent to an elution column. The difference is that the used

column was a C-18 column and that the mobile phase composition was fixed as there was only one compound to elute. The mobile phase was obtained through the mixture of two different solvents: solvent A (5% MeOH in water) and solvent B (95% MeOH in water). Their proportion was 40% of A and 60 % of B.

The dectection of atrazine was done through UV detection at 220 [nm].

3.5.3 COD Cell Test

The COD (chemical oxygen demand) is a measurement of the oxygen required to oxidize soluble and particulate organic matter in water. Higher COD levels mean a greater amount of oxidizable organic material in the sample.

The COD of the samples was determined through the oxidation of the water samples with a hot sulfuric solution of potassium dichromate, with silver sulfate as catalyst. The reactants solution was provided in the form of cells of 2 mL. The WW to be tested was then added in the same proportions (2 mL). The cells were then heated at 148°C for 120 [min] in a preheated thermoreactor, cooled to room temperature before measurement of the samples in a spectrophotometer. This latter determined the concentration of green Cr^{3+} in the samples, before automatically converting the signal in COD $[\frac{mg}{L}]$.

3.5.4 Optical microscopy

Optical microscope Olympus Provis AX70 was used to observe agglomeration of the TiO_2 particulates in laboratory grade water and wastewater. 2 solutions were observed using a 10X power magnifying lens : TiO_2 solution at concentration 1.5 $[\frac{g}{L}]$ diluted in laboratory grade water and TiO_2 solution at concentration 1.5 $[\frac{g}{L}]$ diluted in wastewater.

Chapter 4

Results and discussions

4.1 Kinetics based approach

This section contains the results obtained with the Cytotoxics Degradation Experiment method, which aimed to answer the following question:

- What are the effects of the parameters listed below on antineoplastics degradation kinetics?
  - Presence of catalyst (TiO_2);
  - Laboratory Grade Water (LGW) matrix, wastewater (WW) matrix;
  - LP, MP lamp;
  - Presence of hydrogen peroxide (H_2O_2).

The 8 Cytostatic Degradation Experiments realised to answer this question were presented in table 3.3 of section 3.2.1.

4.1.1 Influence of the catalyst

The influence of the catalyst was first studied in laboratory grade water, under the action of two LP lamps. The graphs 4.1a and 4.1b present the degradation kinetics of the four cytotoxics versus time, without catalyst (on the left) and in presence of catalyst (on the right).

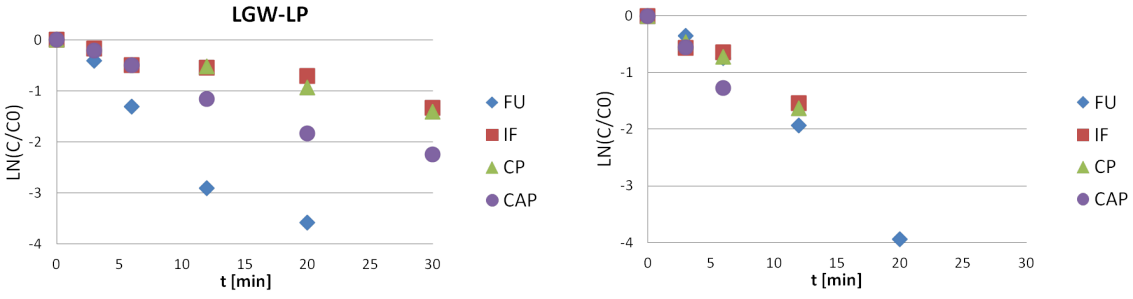

(a) LGW-LP (b) LGW-LP/TiO_2

Figure 4.1: Degradation of cytotoxics over time in LGW in presence and in absence of catalyst

It can be seen on figure 4.1 that, in both cases, all four cytotoxics were degraded following a pseudo-first order degradation kinetics, as the evolution of the concentration of the drugs was

found to follow equations of the type ($R^2 \geq 0.934$) :

$$\log\left(\frac{C}{C_0}\right) = k\ t \tag{4.1}$$

Where C_0 is the initial concentration, k $\left[\frac{1}{min}\right]$ is the pseudo-first order degradation constant and t [min] is the experimental time. The analysis of the control samples kept in the dark during the whole experiment permitted to ensure that the drugs did not degrade without irradiation. The figure 4.2 allows a comparison of the degradation rates of the four cytotoxics with and without catalyst.

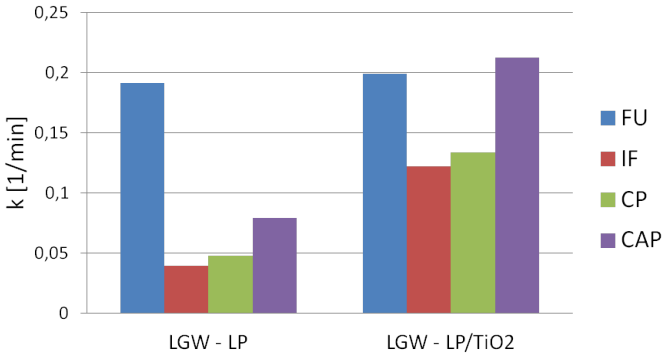

Figure 4.2: Degradation rates of the four studied cytotoxics in LGW, without and in presence of catalyst

The first thing to observe is that photolysis alone permitted to partially degrade the drugs. Then, the lamps seem to efficiently activate the catalyst, as the four drugs presented improved kinetics under the action of this latter. It can be supposed that the presence of the catalyst led to the formation of new reaction pathways, demanding lower activation energies. Also, if the degradation of the drugs is quite unbalanced in absence of catalyst, degradation rates are more uniform after the addition of TiO_2. This could be induced by the fact that the new reaction pathways goes through an intermediate step of hydroxyl radicals production (cfr. section 1.4.2), which often operates a less selective oxidation (similar activation energy for the four compounds) than direct photolysis [57].

4.1.2 Influence of the matrix

To evaluate the influence of the matrix on the degradation kinetics, the same experiments as in section 4.1.1 were performed in wastewater matrix. The graphs 4.3a and 4.3b present the degradation kinetics of the four cytotoxics versus time, without (on the left) and in presence of catalyst (on the right).

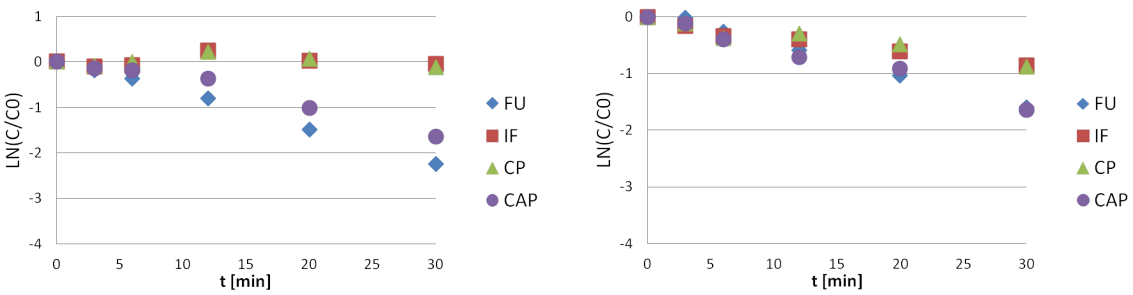

(a) WW-LP (b) WW-LP/TiO_2

Figure 4.3: Degradation of the cytostatics over time, in WW in presence and in absence of catalyst

It can be observed that, neither Ifosfamide nor Cyclophosmamide were degraded in absence of the catalyst. In the other cases, the drugs where degraded following pseudo first-order kinetics ($R^2 \geq 0.91$).

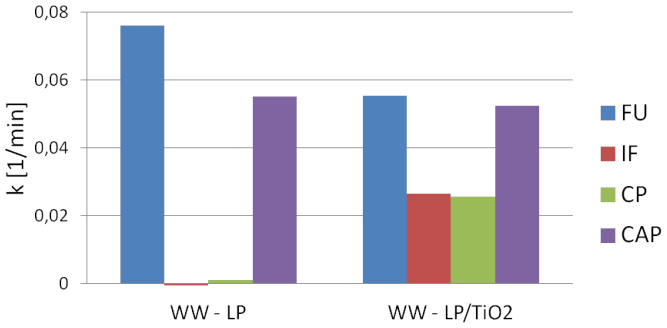

Figure 4.4: Degradation rates of the four studied cytotoxics in WW, without and in presence of catalyst

The same general trend as in LGW was observed in WW (cfr. figure 4.4): the lower activation energies of the reaction pathways induced by the addition of catalyst led to an homogenisation of the degradation rates, and a general improvement of the kinetics.

However, for what concerns 5-Fluorouracil and Capecitabine, it can be observed that the addition of catalyst led to no improvement of the kinetics. This could be explained by the fact that photolysis showed itself already quite efficient to degrade those two compounds, and, as the reaction pathways generated by the catalyst show much closer activation energies, part of the energy that was initially used to degrade 5-Florouracil and Capecitabine were used to degrade Cyclophosphamide and Ifosfamide.

Figure 4.5 displays the degradation rates of the four compounds without catalyst, under irradiation of two LP lamps, in laboratory grade water (on then left) and in wastewater (on the right).

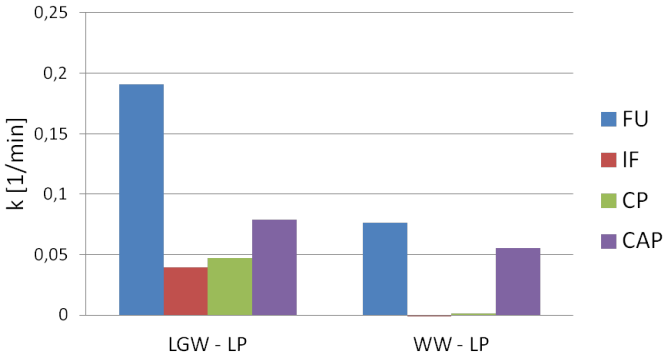

Figure 4.5: Degradation rate of the four studied cytotoxics in LGW and WW, in absence of catalyst and under irradiation of 2 LP lamps

Photolysis kinetics of all four cytotoxics were observed to be slower in wastewater. According to Wang et al [75], this could be due to the presence of humic acid in wastewater, that may hinder the photolysis of target compounds through the absorption of the available light and the scavenging of the free radicals produced. Furthermore, Carbonero et al. [14] suggested that dissolved organic matter could cause comparable inhibition effects.

Similar matrix-induced effects were observed in presence of catalyst. Figure 4.6 displays the degradation rates of the four compounds in presence of catalyst, under irradiation of two LP lamps, in laboratory grade water (on then left) and in wastewater (on the right).

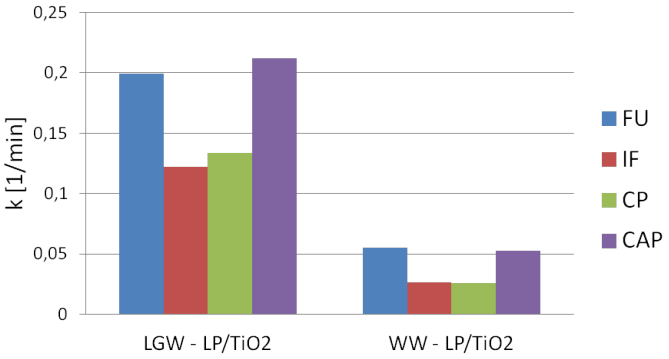

Figure 4.6: Degradation rates of the four studied cytotoxics in LGW and WW, in presence of catalyst and under irradiation of 2 LP lamps

Although a large number of constituents of the WW matrix might influence photocatalytic reactions with the target pharmaceuticals, Carbonaro et al [14] suggested that dissolved organic matter may play a major role in the observed inhibition. The photocatalytic degradation can be affected in various ways [28]: (1) reduction, by competitive scavenging, of the effective $OH^{\bullet}$ concentration available to react with the pharmaceuticals, (2) competitive adsorption on catalyst particulates, and (3) absorption of incident photons, reducing their availability for TiO_2 excitation.

Also, it was observed (cfr. figures 4.7a and 4.7b) that catalyst particulates underwent an increased agglomeration in wastewater compared to their behaviour in laboratory grade water. This could partially explain the observed lower efficiency of the catalyst in wastewater, as

agglomeration permits a much poorer exploitation of the active surface of the catalyst. Indeed, when agglomeration occurs, it leads to a diminution of the active surface available, which implies a reduction of hydroxyl radicals generation and oxidation of the target compounds.

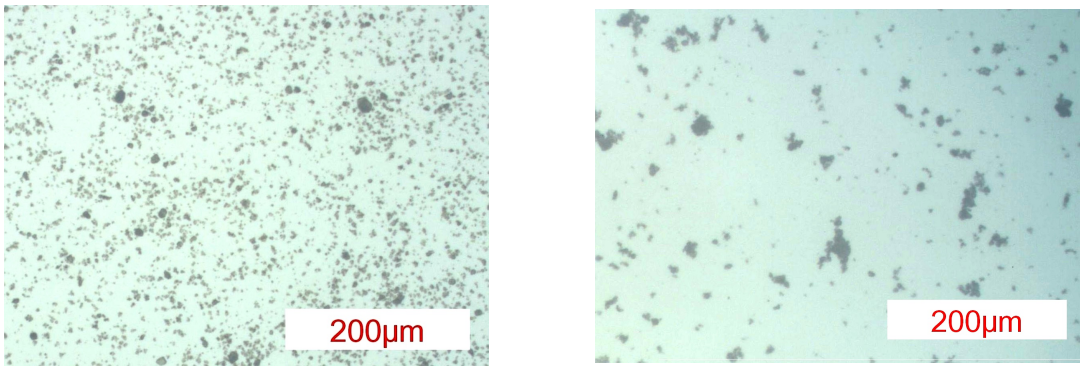

(a) LGW/TiO_2 (b) WW/TiO_2

Figure 4.7: TiO_2 1.5 $\frac{g}{L}$ diluted in laboratory grade water and wastewater. Photos (10X) obtained through optical microscopy

According to Topuz et al. [73], agglomeration of TiO_2 in wastewater is mainly due to (1) the reduction of the energy barrier for stability, induced by the screening of the surface catalyst charge by divalent cations and (2) bridging effects between TiO_2 particulates induced by the presence of natural organic matter (cfr. sections 1.5.4.3 and 1.5.4.4).

4.1.3 Influence of irradiation source

To evaluate the influence of the irradiation source, experiments using MP lamps for direct photolysis and photocalysed degradation of the cytotoxic compounds were performed in wastewater. There were then compared to the similar experiments performed through low pressure lamps irradiation. Figures 4.8a and 4.8b display the evolution of the four cytotoxics concentrations over time through the two MP lamp-based experiments.

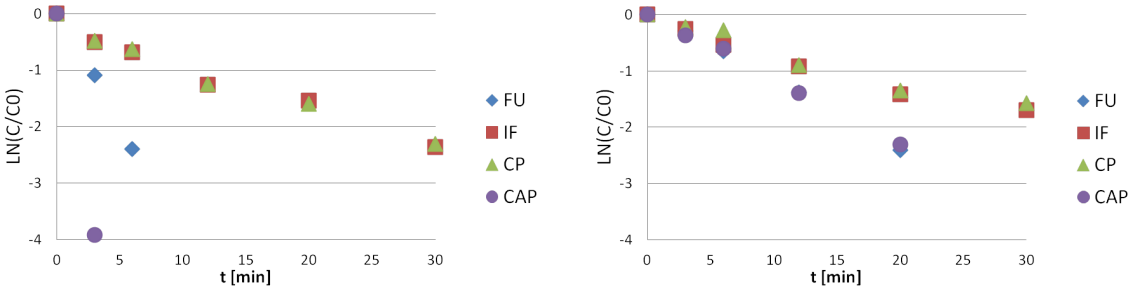

(a) WW-LP (b) WW-MP/TiO_2

Figure 4.8: Degradation of the cytostatics over time in WW through irradiation of one MP lamp, without and in presence of catalyst

In both cases, it was observed that all four cytotoxics underwent pseudo first-order degradation kinetics ($R^2 \geq 0.95$). Figure 4.9 displays the degradation rates obtained through cytotoxics photolysis and photocatalysis under MP lamp irradiation. It appears that the addition of catalyst led to a very different behaviour than when using the LP lamps.

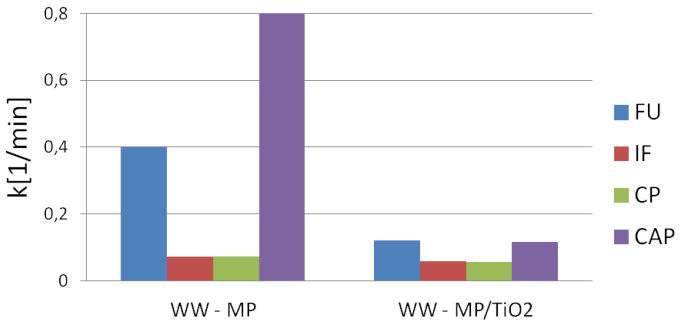

Figure 4.9: Degradation rates of the four studied cytotoxics in WW, without and in presence of catalyst, under irradiation of one MP lamp

Indeed, in presence of the catalyst, the degradation showed much slower kinetics. This could be due to very poor activation of the catalyst particulates by the MP lamp irradiation. As high degradation rates were observed in absence of catalyst, it can be supposed that the predominant mechanism for cytotoxics degradation, under MP lamp irradiation, is direct photolysis. Given the fact that MP lamps show very spread out wavelengths range (cfr. figure 3.2), some wavelengths, efficient to initiate light-induced degradation of the target compounds, might be less efficient towards the catalyst. The poorly-activated TiO_2 particulates would then act as light hindrance, reducing the efficiency of the process.

However, when compared to processes using LP lamps, the degradation rates obtained with the MP lamp remain much higher. This can be observed on figure 4.10, which compares the degradation rates obtained through LP-based photocatalysis (more efficient than LP-based photolysis as observed before) with the two processes performed under the irradiation of the MP lamp.

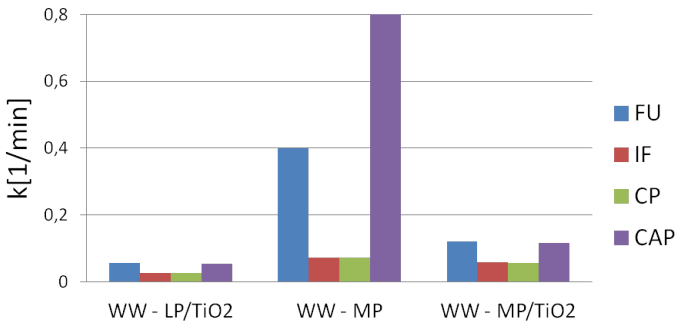

Figure 4.10: Comparison of the degradation rates of LP-based photocatalysis with MP-based photolysis and photocatalysis

This could be induced by the difference in power between the two lamps (10 [W] for the LP lamp and 125 [W] for the MP lamp). This will be further investigated through the energy based approach. Based on degradation kinetics only, photolysis under MP lamp irradiation seems to be the most efficient of the processes studied until now.

4.1.4 Comparison of TiO_2-based processes and H_2O_2-based processes

As introduced in section 1.2, H_2O_2 have been widely used in wastewater treatment. Two additional experiments were then performed in order to compare the efficiency of the TiO_2-based and H_2O_2-based treatments. The two experiments were performed under irradiation of two LP lamps.

In the first one, peroxide was added at the beginning of the experiment, instead of catalyst. In the second one, both peroxide and catalyst were added at the beginning of the experiment, in order to evaluate the possibility to combine the two reactants. Figure 4.11a and 4.11b present the evolution of the target pollutants concentration over time for both processes.

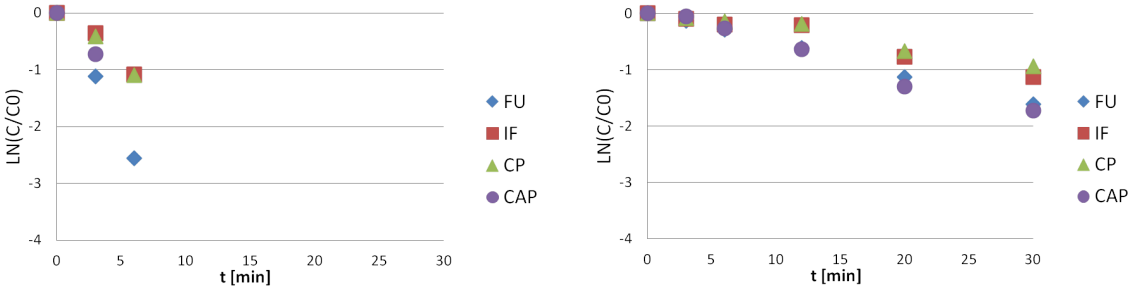

(a) WW-LP/H_2O_2 (b) WW-LP/H_2O_2/TiO_2

Figure 4.11: Degradation of the cytostatics over time in WW through irradiation of one MP lamp, without and in presence of catalyst

Both experiments showed pseudo first-order kinetics of the four cytotoxics ($R^2 \geq 0.95$). The figure 4.12 compares the degradation rates obtained with H_2O_2 alone and with both H_2O_2 and TiO_2, under irradiation of LP lamps.

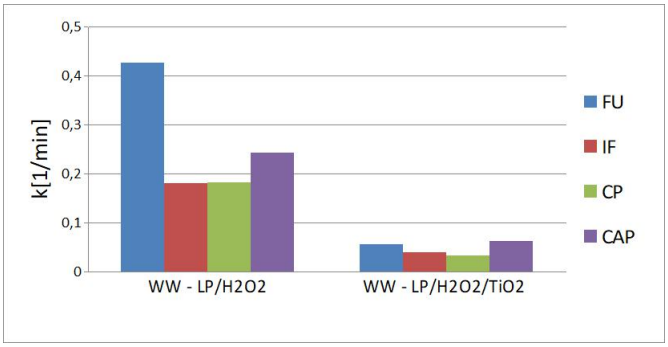

Figure 4.12: Degradation rates of the four studied cytotoxics in WW, in presence of H_2O_2 alone (left) and in presence of both H_2O_2 and TiO_2 (right), under irradiation of two LP lamps

It can be observed on figure 4.12 that degradation in presence of H_2O_2 alone presented much higher degradation rates than degradation in presence of the combination of the two reactants. Several suppositions can be made based on these observations: (1) in presence of H_2O_2 alone, the predominant mechanism of the cytotoxics degradation goes through a very efficient formation of hydroxyl radicals by peroxides homolitic cleavage under irradiation and (2) peroxide and catalyst seemed to exercise inhibition on each other. According to Sahel et al. [65], H_2O_2 can adsorb on TiO_2 particulates under variate conditions, which could explain this inter-inhibition.

Based on those results, it can be concluded that combining TiO_2 and H_2O_2 is not an efficient option, as it implies a more complex process for lower degradation efficiency.

Figure 4.13 proposes a comparison of the degradation rates of the four cytotoxics through H_2O_2-photolysis (left) and photocatalysis (right), under LP lamps irradiation.

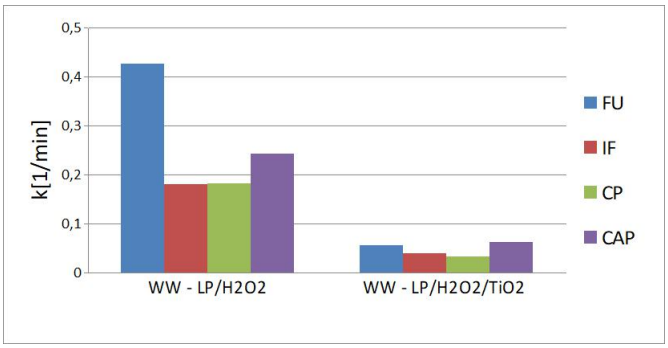

Figure 4.13: Degradation rates of the four studied cytotoxics in WW, in presence of H_2O_2 (left) and TiO_2 (right), under irradiation of 2 LP lamps

H_2O_2-photolysis showed higher degradation rates than photocatalysis, which could be due a more efficient hydroxyl radicals formation through hydrogen peroxide cleavage than through photocatalyst particulates activation. Table 4.1 displays the reduction of the COD through all the experiments performed with wastewater. It can be seen that, in addition to propose a more efficient cytotoxics degradation, H_2O_2-photolysis also showed the highest COD reduction.

N°	**Name**	$\frac{COD_0 - COD_f}{COD_0} \cdot 100\%$
3	WW - LP	0.85 ± 0
4	WW - LP/TiO_2	1.71 ± 0
5	WW - MP	2.54 ± 0
6	WW - MP/TiO_2	4.3 ± 1.7
7	WW - LP/H_2O_2	11.3 ± 0.5
8	WW - LP/H_2O_2/TiO_2	10.5 ± 0.3

Table 4.1: Reduction of the Chemical Oxygen Demand in % through all the experiments performed with wastewater

Finally, figure 4.14 displays the degradation rates obtained through all the studied processes performed in wastewater.

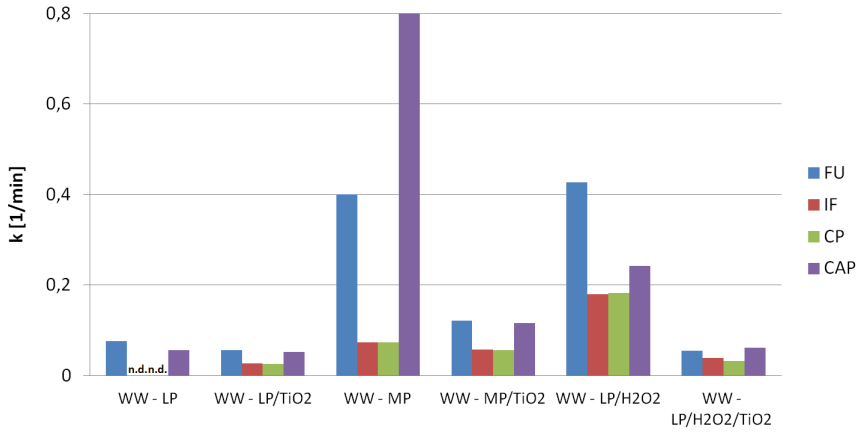

Figure 4.14: Degradation rates obtained through all the studied processes performed in wastewater. n.d. states for "not degraded".

On a degradation kinetics basis, it can be concluded that the H_2O_2-based process appears to be the most efficient. The only process that seems to compete with the H_2O_2-based process is the photolysis process under MP lamp irradiation. However, those two processes used irradiation source of very different power. It would then be interesting to compare the processes through an energy based approach, which will be developed in the next section.

4.2 Energy based approach

The energy based evaluation aimed to compare the different processes in terms of energy needed to degrade the target compounds by one order of magnitude. As the used set-up might greatly influence the energy consumption of the process, it was decided to base the energy consumption comparison on a smaller scale: it is the energy needed to be sent to the solution that was taken into account in the calculations.

Two steps were needed to perform this evaluation, (i) the determination, by Atrazine Actinometry, of the rate of energy, emitted by the low pressure (LP) UV lamp and the medium pressure (MP) UV lamp, that is usable to degrade the drugs and (ii) the calculation of the amount of energy that needs to reach the drugs molecules in order to reduce their concentration by one order of magnitude, which was done through Fluence-based EEO Calculation.

4.2.1 Atrazine Actinometry

The results obtained by Atrazine Actinometry, for the characterisation of the Fluence rates generated by one LP lamp, two LP lamp and one MP lamp are presented of figure 4.15.

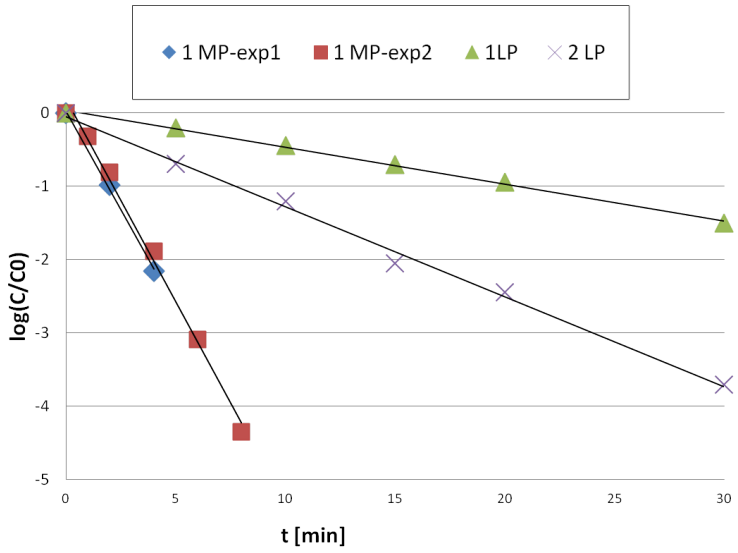

Figure 4.15: Degradations of Atrazine through irradiation of one LP lamp, two LP lamp and one MP lamp

As expected, degradation showed pseudo first-order kinetics. The degradation rates, as well as the Fluence rates obtained through the Atrazine Actinometry experiment are presented in table 4.2:

Experiment	k $\left[\frac{1}{min}\right]$	R^2	Fluence rate $\left[\frac{Einstein}{s\ L}\right]$	Fluence rate $\left[\frac{J}{s\ L}\right]$
1 MP-exp1	0.54	0.998	$2.5\ \ 10^{-7}$	$1.2\ 10^{-7}$
1 MP-exp2	0.55	0.994	$2\ \ 10^{-7}$	$9.5\ 10^{-8}$
1 LP	0.05	0.997	$4\ \ 10^{-7}$	$1.9\ \ 10^{-10}$
2 LP	0.12	0.995	$5\ \ 10^{-7}$	$2.4\ \ 10^{-10}$

Table 4.2: Degradation rates and Fluence rates obtained through Atrazine Actinometry

In the literature, Fluence rates are often expressed in $\left[\frac{Einstein}{s\ cm^2}\right]$. Table 4.3 displays the Fluence rates obtained converted in these units.

Lamp system	Fluence rate $\left[\frac{Einstein}{s\ cm^2}\right]$
One medium pressure lamp	$6.4\ \ 10^{-9} \pm 7.5\ 10^{-10}$
One low pressure lamp	$1.15\ \ 10^{-9}$
Two low pressure lamp	$7.2\ \ 10^{-10}$

Table 4.3: Fluence rates obtained through Atrazine Actinometry in $\left[\frac{Einstein}{s\ cm^2}\right]$

Rosenfeldt at al. [63] found Fluence rates values of $9.3\ \ 10^{-9}\ \left[\frac{Einstein}{s\ cm^2}\right]$ for a medium pressure lamp of power 150 [W] and $4.55\ \ 10^{-9}\ \left[\frac{Einstein}{s\ cm^2}\right]$ for a low pressure lamp of power 15 [W], by Atrazine Actinometry experiments performed in a 500 mL batch reactor. The results found experimentally (cfr figure 4.3) seem consistent when compared with these values, since they showed in both cases the same order of magnitude. Dobaradaran et al. [27] found a Fluence rate value of $6.01\ \ 10^{-9}\ \left[\frac{Einstein}{s\ cm^2}\right]$ for a low pressure lamp of power 15 [W]. This value is about 5 times greater than the one obtained through the present study (cfr. table 4.3), but also remains in the same order of magnitude.

4.2.2 Fluence-based EEO calculations

The Fluence rates obtained through Atrazine actinometry were used to calculate the Fluence-based EEO for the different studied processes and operating conditions. The results are displayed on figure 4.16:

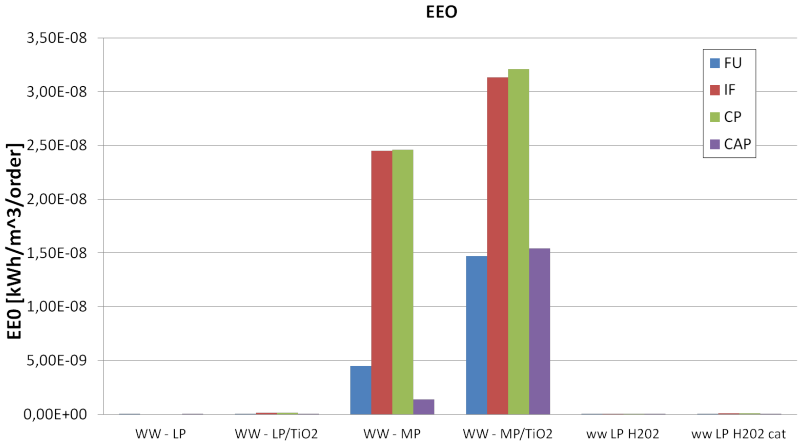

Figure 4.16: Fluence-based EEO of the studied processes

The first thing to observe is that processes using the MP lamps showed much higher EEO. Although MP-photolysis proposed competitive degradation rates, it appeared to be much less energy efficient than LP-based processes. Figure 4.17 proposes the exact same results as figure 4.16, but at a smaller scale, which is more convenient in order to compare the energy efficiency of the LP-based processes.

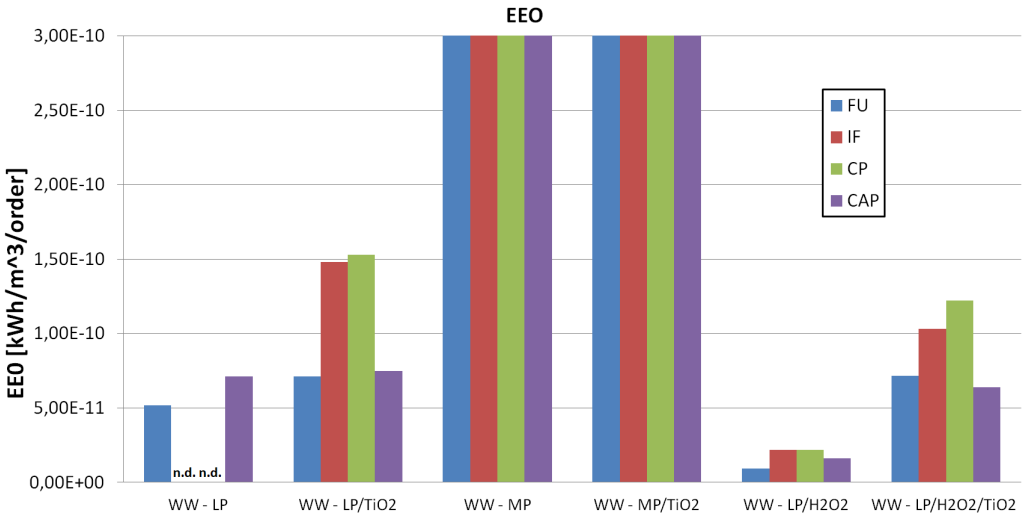

Figure 4.17: Fluence-based EEO of the studied processes. "n.d." states for "not degraded"

EEO were calculated as a function of the Fluence rate, the degradation rate and the volume of the reactor vessel (cfr. equation 3.9). As the same lamps and set-up were used for all the LP-based processes, the differences between their calculated EEO values is only a function of the degradation rates. The Lp-based processes that showed the best kinetics efficiency are then logically also more energy-efficient.

Finally, we can conclude that, from both kinetics-based and energy-based approaches, the H_2O_2-based process appeared to be the most efficient. The TiO_2-based photocatalytic degradation under LP lamp irradiation remains however a feasible option, as it showed improved kinetics and energy efficiency compared to direct LP-photolysis and theoretical time to decrease the concentration of all four cytotoxics by one order of magnitude of less than 90 minutes (the details of the calculation will be introduced in the next section).

TiO_2-based and H_2O_2-based processes use different reactants, which might induce different post-treatments of these reactants, different set-ups and thus different costs. Since price is often a primary criterion in the selection of industrial processes, it would be interesting to evaluate the costs linked to the TiO_2-based and H_2O_2-based processes. A primary economic evaluation of those two processes will be developed in the next section.

4.3 Economic approach

The economic approach aimed to compare, on an economic basis, the two most promising processes that were brought out as a result of the two first approaches, namely the TiO_2-based photocatalytic degradation and the H_2O_2-based degradation, both underwent under LP lamps irradiation. One of the central aspect of this evaluation is the duration of the treatment, calculated (cfr. equation 3.10) as the time needed to decrease the concentration of the slower-degrading drug by one order of magnitude:

Process	**HRT [min]**
WW - LP/TiO_2	88.56
WW - LP/H_2O_2	12.8

Table 4.4: HRT values

Each process was separated into two steps in order to perform the economic evaluation: the degradation part, which is similar for both processes, and the treatment needed to handle the reactants after the degradation, namely filtration for the TiO_2 and radicals quenching for the H_2O_2.

The aspects to take into account in the degradation part are: the supply of the reactants, the replacement of the lamps and the energy supply for the duration of the treatment. Table 4.5 and 4.6 resume the items and prices included in this first part:

Item	**Price**
TiO_2 $\left[\frac{\$}{g\ min}\right]$	$3.6\ 10^{-5}$
Lamp $\left[\frac{\$}{min}\right]$	$1.4\ 10^{-4}$
Energy $\left[\frac{\$}{kWh}\right]$ [71]	0.28

Table 4.5: WW - LP/TiO_2

Item	**Price**
H_2O_2 $\left[\frac{\$}{g}\right]$	$6\ 10^{-3}$
Lamp $\left[\frac{\$}{min}\right]$	$1.4\ 10^{-4}$
Energy $\left[\frac{\$}{kWh}\right]$ [71]	0.28

Table 4.6: WW - LP/H_2O_2

Table 4.7: Items and prices included in the degradation part of the treatments

The catalyst price in $\left[\frac{\$}{g\ min}\right]$ was calculated based on its price per [g] (0.13 $\left[\frac{\$}{g}\right]$ supplied by Alibaba Group) and its mean lifetime in a photocatalysis system. A 60 hours lifetime was supposed for catalyst particulates, based on the work of Janus et al. [39]. The same reasoning was applied to calculate lamps price in $\left[\frac{\$}{min}\right]$. Price (67 \$) and lifetime (8000 hours) of the lamps were provided by the supplier (Helios Quartz). Two lamps of 10 [W] were supposed to be used, which gives a total input power of 20 [W] to be provided for the two processes.

The post-treatment of the TiO_2 particulates was supposed to consist in filtration induced by a pump, through a one-channel Filtanium 100 kD membrane provided by TAMI Industries, which is a membrane that has been studied by the research team. The costs of the membranes was calculated based on their price in $\left[\frac{\$}{m^2}\right]$ and their average lifetime (400 hours), provided by the supplier.

An important step in the economic evaluation of the filtration is the determination of the maximal transmembrane flux needed to obtain the HRT. It is simply done by dividing the volume

of the reactor vessel by the HRT, as in equation 4.2:

$$Flux_{max} = \frac{V}{HRT} = 0.0147 \left[\frac{L}{min}\right] \tag{4.2}$$

Based on the specifications provided by the supplier, the membrane surface needed to reach this flux (11.8 $[cm^2]$) was determined for a pump working at 2.5 [bars]. A typical power input needed to supply such a pump was then determined to be of 30 [W] [72]. Table 4.8 resumes the items and prices included in the filtration part.

Item	**Price**
Membrane $\left[\frac{\$}{m^2\ min}\right]$	0.16
Energy $\left[\frac{\$}{kWh}\right]$ [71]	0.28

Table 4.8: Items and costs included in the filtration step

The post treatment of the H_2O_2 was supposed to consist in quenching by catalase, a method which was suggested by Liu et al. [50]. A catalase concentration of 0.2 $\left[\frac{mg}{L}\right]$ was selected, as it is, according to their work, sufficient to degrade 100 [ppm] of hydrogen peroxide in less than 10 [min]. The only item included in the quenching part is then catalase, for which a cost of 0.005 $\left[\frac{\$}{g}\right]$ was supposed (supplied by Alibaba Group).

Figure 4.18 displays the overall costs of the two processes, for the treatment of $1m^3$ of wastewater, and the diminution of the drugs concentration by one order of magnitude.

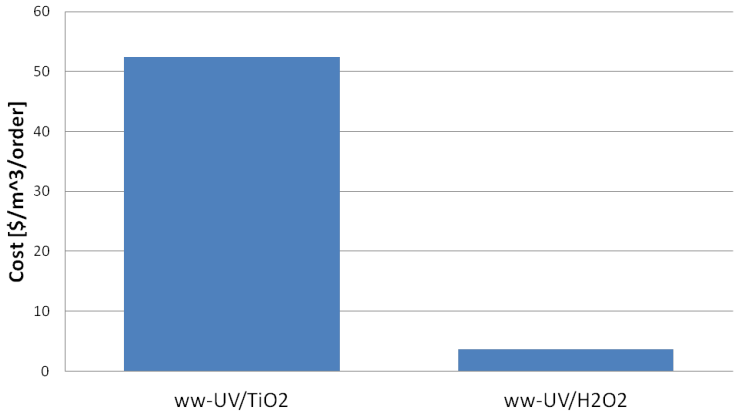

Figure 4.18: Relative importance of the different cost categories [%]

According to this preliminary economic evaluation, TiO_2-based process would cost nearly fifteen times more than the H_2O_2-based process. Figure 4.19 permits to compare the relative importance of the different cost categories related to those two processes.

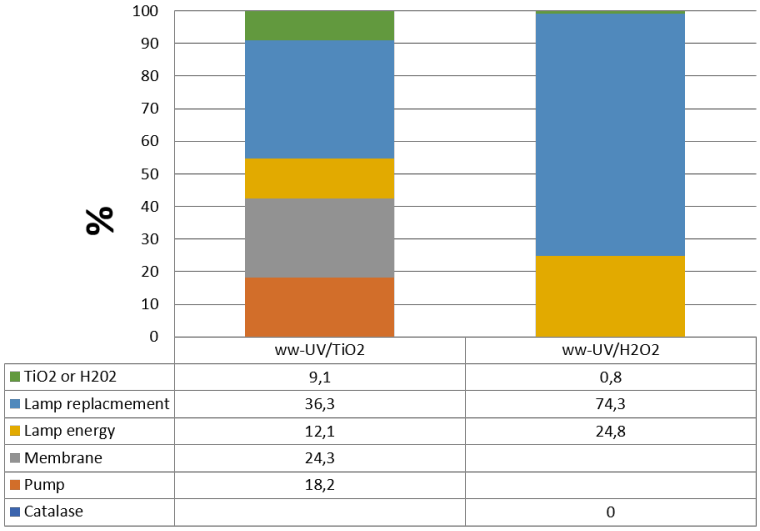

	ww-UV/TiO2	ww-UV/H2O2
TiO2 or H202	9,1	0,8
Lamp replacmement	36,3	74,3
Lamp energy	12,1	24,8
Membrane	24,3	
Pump	18,2	
Catalase		0

Figure 4.19: Relative importance of the different cost categories [%]

It appears that, in both cases, the most important costs are related to the lamp replacement. A way to decrease those costs would be to use LEDs, which propose lower prices and lower energy demand [15][37]. The supply of the catalyst or peroxide represents the lower costs in both cases, although it represents nearly 10 % in the case of the TiO_2-based process for less that 1 % in the case of the H_2O_2-based process. Also, while the degradation part of the treatment represents only 57.5 % of the overall cost in the case of the TiO_2-based process, it represents nearly 100 % percent in the case of the H_2O_2-based process (cfr. figure 4.20).

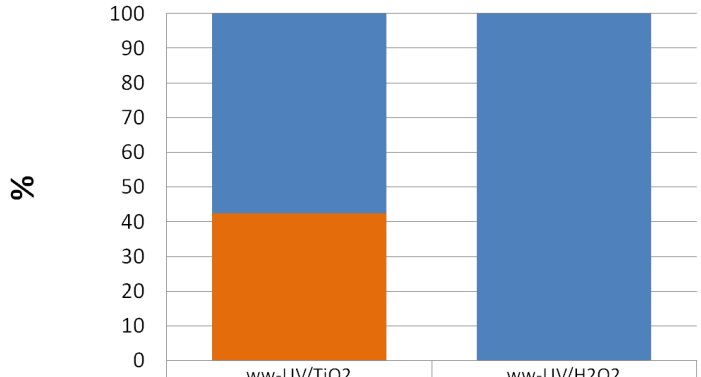

	ww-UV/TiO2	ww-UV/H2O2
Degradation part	57,5	99,97
Reactants post-treatment	42,5	0,03

Figure 4.20: Relative importance of the degradation and reactants handling parts of the treatments [%]

Finally, we can conclude that the PMR system is more expensive that the UV/H_2O_2, mostly due to the longer duration needed for the treatment and the price of the filtration step which is much higher than the price of the peroxide quenching. However, it is to be kept in mind that this is only a preliminary economic evaluation, performed to give an idea of the costs linked to the two processes. Further studies, performed at larger scales, are still needed to enlighten the dark points persisting in this evaluation, such as investment costs and maintenance.

Chapter 5

Recommendations for future research

This section aims to enlighten the limitations of this work and provide further lines of inquiry for future researches. This will be done by first investigating the possibilities of improving operating conditions, then by proposing future research steps that should be considered.

Further optimisation of the operating conditions of the photocatalytic process

If the feasibility of the photocatalytic process has been shown through the present research, there are still parameters that need to be investigated which could lead to further improvement of the process.

The first aspect that should be further investigated is the optimisation of the catalyst load. Indeed, the catalyst concentration which has been used to study the photocatalytic process performances is based on an optimisation study performed in laboratory grade water. As numerous inhibition effects of the wastewater matrix, in comparison to degradation in laboratory grade water, were pointed out in this work, the optimal catalyst load for cytotoxic degradation is likely to be different in wastewater. As the treatment is actually performed on wastewater, a catalyst load obtained through optimisation in wastewater matrix would be preferable in order to maximise the efficiency of the process.

Another aspect which has not been taken into consideration in this work is the influence of temperature. Indeed, all experiments were performed at room temperature. Abdel-Aal et al. [1] predicted the downstream wastewater temperatures of 5 wastewater treatment plants located in Belgium. They obtained temperatures comprised between 5 řC in winter and 23 in summer. Supposing that this range of temperature is representative of the typical temperature range of WWTP effluents, it would be interesting to evaluate the influence of these temperatures on the treatment efficiency.

Also, studies have shown the beneficial effects of aeration on hydroxyl radicals production and photocatalytic degradation [78] [55] [21]. As seen in section 1.5.6 of chapter 1, an optimisation of the O_2 concentration is possible and likely to act favourably on the photocatalytic degradation

efficiency [78].

Finally, this work is based on the use of conventional mercury vapour lamps as UV irradiation source, which have been largely studied [20]. However, the number of publications reporting photocatalytic applications based on LED light sources is increasing each year [69], showing the potential benefits of the latter, such as higher electricity to luminous energy conversion efficiency, longer lifetimes and adaptable output wavelength [51]. Further investigations would be interesting in order to evaluate the feasibility of using LED light sources in our specific study case, namely photocatalytic degradation of antineoplastic compounds. Another lead that could be followed is the possibility to harvest sunlight to decrease the energy cost of the process. Kumar et Devi [43] investigated the possibility to take advantage of both sunlight and UV light for photocatalysis using modified TiO_2.

Next research steps to be considered

Throughout this work, photocatalytic degradation in batch operation was studied. The logical next step is to study the implementation of the photocatalytic degradation in a continuous process that combines degradation of the drugs and confinement of the catalyst in the system using a membrane module, i.e. continuous photocatalyic membrane reactors. A possible experimental set-up, used by Sarasidis et al. [67] for their study, is displayed on figure 5.1.

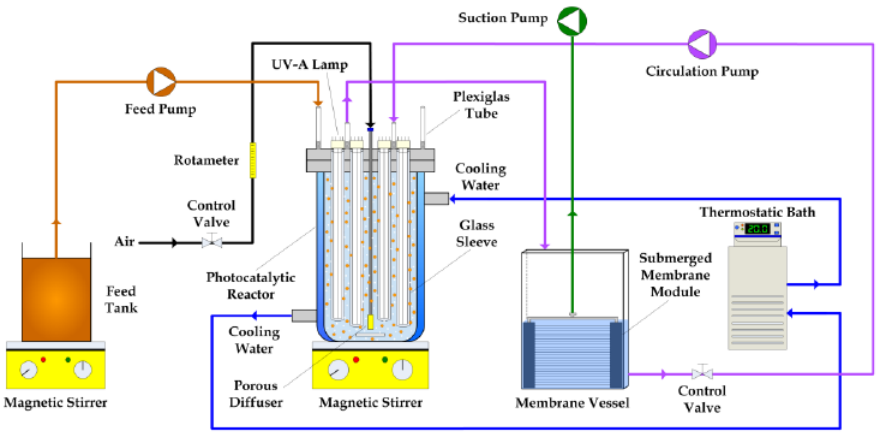

Figure 5.1: Laboratory continuous PMR system used by and reprinted from Sarasidis et al. [67]

The main differences with the set-up used for the present study are the alimentation of the reactor from a separated feed tank through an alimentation pump, the presence of a filtration module, the recirculation of the retentate through a circulation pump, and the recuperation of the treated permeate with the help of a suction pump.

Another interesting is a Life Cycle Analysis (LCA) of the whole process. It would provide a precise energy costs assessment and an economic evaluation at larger scale than the one conducted in the present study. It also allows to obtain an assessment of the sustainability of the treatment, another important parameter to consider when choosing an industrial process, which has not been developed in this work. This would be interesting to evaluate since hydrogen peroxide is almost exclusively produced through the anthraquinone process, a multistep method requiring significant energy input and generating waste [13].

Conclusions

Throughout the present document, the potential of UV-photocatalytic degradation as treatment technology for the elimination of anti-cancer drugs was assessed, and compared to direct UV-photolysis and UV/H_2O_2-photolysis. The study was conducted for varying operating conditions (matrix and irradiation source) through a triple approach: (i) degradation kinetics (ii) energy consumption and (iii) costs assessment.

Three main conclusions were pointed out from the first approach. First of all, while photocatalysis is more efficient than direct photolysis using low pressure (LP) mercury lamps as irradiation source, it is direct photolysis that is more efficient when using medium (MP) pressure mercury lamps. Secondly, MP-based photolysis and photocatalysis were concluded to present higher kinetics-based efficiency than LP-based photolysis and photocatalysis, due to the higher energy output of the irradiation source. Finally, if direct photolysis and photocatalysis have been shown to be able to degrade the drugs when using the adequate irradiation source, it is UV/H_2O_2-photolysis under LP lamp irradiation that was concluded to be the most efficient based on degradation kinetics. In addition, wastewater matrix was concluded to cause inhibition effects on both direct photolysis and photocatalysis, due to its numerous additional components when compared to LGW, and the enhanced TiO_2 particulates agglomeration in WW.

The second approach allowed to conclude that MP-based processes are much less energy efficient than LP-based processes, which means that preference must be given to photocatalyis or UV/H_2O_2-photolysis if energy consumption is the primary concern. Again, UV/H_2O_2-photolysis appeared to be more efficient than any other studied process, based on energy demands.

Through the third approach, UV/H_2O_2-photolysis was shown to be cheaper than photocatalysis, mainly due to the filtration step and longer treatment duration needed for the latter.

From those three approaches, it finally results that, although photocatalysis appeared to be conceivable, the most promising process remains UV/H_2O_2-photolysis. This is however to be taken with caution, as further optimisation of the photocatalysic degradation are still possible, and the economic evaluation that was performed only consists in a primary evaluation with limited scale. Furthermore, sustainability evaluation of the processes, which is often of primary concern when choosing industrial processes, was not investigated through this work.

Bibliography

[1] M. Abdel-Aal, M. Mohamed, R. Smits, R. E. Abdel-Aal, K. De Gussem, A. Schellart, and S. Tait. Predicting wastewater temperatures in sewer pipes using abductive network models. *Water Science Technology*, 71:89–96, 2015.

[2] Khan Academy. "enzymes review". https://www.khanacademy.org/science/high-school-biology/hs-energy-and-transport/hs-enzymes/a/hs-enzymes-review.

[3] R. Andreozzi, V. Caprio, A. Insola, and R. Marotta. Advanced oxidation processes (aop) for water purification and recovery. *Catalysis Today*, 53:51–59, 1999.

[4] S. Ardizzone, C. L. Bianchi, G. Cappelletti, S. Gialanella, C. Pirola, and V. Ragaini. Tailored anatase/brookite nanocrystalline tio2 :the optimal particle features for liquid- and gas-phase photocatalytic reactions. *J. Phys. Chem. C*, 111:13222–13231, 2007.

[5] P. Asaithambi, E. Alemayehu, B. Sajjadi, and A. R. A. Aziz. Electrical energy per order determination for the removal pollutant from industrial wastewater using uv/fe2+/h2o2 process: Optimization by response surface methodology. *Water Resources and Industry*, 18:17–32, 2017.

[6] P. W. Atkins, L. Jones, and L. Laverman. *Principes de Chimie*. De Boeck Supérieur, 2014.

[7] K. Azrague, P. Aimar, F. Benoit-Marquie, and M. Maurette. A new combination of a membrane and a photocatalytic reactor for the depollution of turbid water. *Appl. Catal. B: Environ*, 72:197–204, 2007.

[8] S. J. Bell. *The effect of light intensity and temperature on photocatalytic water splitting (phdtheis)*. PhD thesis, Queensland University of Technology, 2011.

[9] F. J. Beltran, G. Ovejero, and B. Acedo. Oxidation of atrazine in water by ultraviolet radiation combined with hydrogen peroxide. *Water Research*, 27(6):1013–1021, 1993.

[10] J.-p. Besse, C. Kausch-Barreto, and J. Garric. Exposure assessment of pharmaceuticals and their metabolites in the aquatic environment: Application to the french situation and preliminary prioritization. *Human and Ecological Risk Assessment: An International Journal*, 14:665–695, 2008.

[11] J. R. Bolton and M. I. Stefan. Fundamental photochemical approach to the concepts of fluence (uv dose) and electrical energy efficiency in photochemical degradation reactions. *Research on Chemical Intermediates*, 28(7-9):857–870, 2002.

[12] G. Camera-Roda and F. Santarelli. Intensification of water detoxification by integrating photocatalysis and pervaporation. *J. Sol. Energy Eng.*, 129:68–73, 2005.

[13] J. M. Campos-Martin, G. Blanco-Brieva, and J. L. G. Fierro. Hydrogen peroxide synthesis: An outlook beyond the anthraquinone process. *Angewandte Chemie International Edition*, 45:6962–6984, 2006.

[14] S. Carbonaro, M. N. Sugihara, and T.J. Strathmann. Continuous-flow photocatalytic treatment of pharmaceutical micropollutants: Activity, inhibition, and deactivation of tio2 photocatalysts in wastewater effluent. *Applied Catalysis B: Environmental*, 129:1–12, 2013.

[15] C. Casado, R. Timmers, A. Sergejevs, C. T. Clarke, D. W. E. Allsopp, C. R. Bowen, R. van Grieken, and J. Marugon. Design and validation of a led-based high intensity photocatalytic reactor for quantifying activity measurements. *Chemical Engineering Journal*, 327:1043–1055, 2017.

[16] Y. Cass and C. F. Musgrave. Guidelines for the safe handling of excreta contaminated by cytotoxic agents. *American Journal of Hospital Pharmacy*, 49:1957–1958, 1992.

[17] S. Chakrabarti. *Solar Photocatalysis for Environmental Remediation.* The Energy and Resources Institute (TERI), 2017.

[18] S. Chakrabarti and B. K. Dutta. Photocatalytic degradation of model textile dyes in wastewater using zno as semiconductor catalyst. *Journal of Hazardous Materials*, 112:269–278, 2004.

[19] M. Cheng, G. Zeng, D. Huang, C. Lai, P. Xu, C. Zhang, and Y. Liu. Hydroxyl radicals based advanced oxidation processes (aops) for remediation of soils contaminated with organic compounds: A review. *Chemical Engineering Journal*, 284:582–598, 2016.

[20] A.-c. Chevremont, J.-l. Boudenne, B. Coulomb, and A.-m. Farnet. Fate of carbamazepine and anthracene in soils watered with uv-led treated wastewaters. *Water Research*, 47:6574–6584, 2013.

[21] S. S. Chin, T. M. Lim, K. Chiang, and A. G. Fane. Factors affecting the performance of a low-pressure submerged membrane photocatalytic reactor. *Chemical Engineering Journal*, 130:53–63, 2007.

[22] AFFSAPS. Agence Française de Sécurité Sanitaire des Produits de Santé. French consumption amounts for pharmaceuticals, including anticancer drugs (atc class l01) for year 2004. 2006.

[23] AFFSAPS. Agence Française de Sécurité Sanitaire des Produits de Santé. French consumption amounts for pharmaceuticals, including anticancer drugs (atc class l01) for year 2008. 2009.

[24] J. G. Derks. *Degradation of organic micropollutants by advanced oxidation through UV/H2O2 (phdthesis).* PhD thesis, Delft University of Technology, 2011.

[25] R. Dewil, D. Mantzavinos, I. Poulios, and M. A. Rodrigo. New perspectives for advanced oxidation processes. *Journal of Environmental Management*, 195:93–99, 2017.

[26] A. Di Paola, E. Garcia-Lopez, G. Marci, and L. Palmisano. A survey of photocatalytic materials for environmental remediation. *Journal of Hazardous Materials*, 211-212:3–29, 2012.

[27] S. Dobaradaran, H. Lutze, A. Mahvi, and T. C. Schmidt. Transformation efficiency and formation of transformation products during photochemical degradation of tce and pce at micromolar concentrations. *Journal of Environmental Health Science and Engineering*, 12:16–26, 2014.

[28] T. E. Doll and F. H. Frimmel. Photocatalytic degradation of carbamazepine, clofibric acid and iomeprol with p25 and hombikat uv100 in the presence of natural organic matter (nom) and other organic water constituents. *Water Research*, 39(2-3):403–411, 2005.

[29] V. Geissen, H. Mol, E. Klumpp, G. Umlauf, M. Nadal, M. van der Ploeg, S. E. A. T. M. van de Zee, and C. J. Ritsema. Emerging pollutants in the environment: A challenge for water resource management. *International Soil and Water Conservation Research*, 3:57–65, 2015.

[30] N. Guichard, D. Guillarme, P. Bonnabry, and S. Fleury-Souverain. Antineoplastic drugs and their analysis: a state of the art review. *Analyst*, 142:2273–2321, 2017.

[31] B. Halling-Sorensen, S. Nors Nielsen, P. F. Lanzky, F. Ingerslev, H. C. Holten Lutzhoft, and S.E. Jorgensen. Occurrence, fate and effects of pharmaceutical substances in the environment-a review. *Chemosphere*, 36:357393, 1998.

[32] J. Harris and L. Dodds. Handling waste from patients receiving cytotoxic drugs. *Pharmaceutical Journal*, 235:289–291, 1985.

[33] J. Herrmann. Heterogeneous photocatalysis: fundamentals and applications to the removal of various types of aqueous pollutants. *Catalysis Today*, 53:115–129, 1999.

[34] C. Hignite and D. L. Azarnoff. Drugs and drug metabolites as environmental contaminants: Chlorophenoxyisobutyrate and salicylic acid in sewage water effluent. *Life Sciences*, 20:337–341, 1977.

[35] G. F. IJpelaar, D. J. H. Harmsen, E. F. Beerendonk, R. C. van Leerdam, D. H. Metz, A. H. Knol, A. Fulmer, and S. Krijnen. Comparison of low pressure and medium pressure uv lamps for uv/h2o2 treatment of natural waters containing micro pollutants. *Ozone: Science Engineering*, 32:329–337, 2010.

[36] IUPAC. "iupac gold book, fluence rate". https://goldbook.iupac.org/html/F/FT07376.html.

[37] M. Izadifard, G. Achari, and C. Langford. Application of photocatalysts and led light sources in drinking water treatment. *Catalysts*, 3:726–743, 2013.

[38] R. Janssens, M. Kanti Mandal, K. Dubey, and P. Luis. Slurry photocatalytic membrane reactor technology for removal of pharmaceutical compounds from wastewater: Towards cytostatic drug elimination. *Science of The Total Environmen*, 599:612–626, 2017.

[39] M. Janus, E. Kusiak-Nejman, J. Choina, and A. Morawski. Lifetime of carbon-modified tio2 photocatalysts under uv light irradiation. *Catalysis Letters*, 131:606–611, 2009.

[40] O. S. Keen, A. D. Dotson, and K. G. Linden. Evaluation of hydrogen peroxide chemical quenching agents following an advanced oxidation process. *Journal of Environmental Engineering*, 139:137–140, 2013.

[41] S. H. Kim, S. W. Lee, G. M. Lee, B.-t. Lee, S.-t. Yun, and S.-o. Kim. Monitoring of tio2-catalytic uv-led photo-oxidation of cyanide contained in mine wastewater and leachate. *Chemosphere*, 143:106–114, 2016.

[42] H. J. Kuhn, S. E. Braslavsky, and R. Schmidt. Chemical actinometry (iupac technical report). *Pure and Applied Chemistry*, 76(12):2105–2146, 2004.

[43] S. G. Kumar and L. G. Devi. Review on modified tio2 photocatalysis under uv/visible light: Selected results and related mechanisms on interfacial charge carrier transfer dynamics. *The Journal of Physical Chemistry A*, 115(46):13211–13241, 2011.

[44] K. Kümmerer. Drugs in the environment: emission of drugs, diagnostic aids and disinfectants into wastewater by hospitals in relation to other sources–a review. *Chemosphere*, 45:957–969, 2001.

[45] K. Kümmerer, A. Haib, A. Schuster, A. Hein, and I. Ebert. Antineoplastic compounds in the environment-substances of special concern. *Environmental Science and Pollution Research International*, 23:14791–14804, 2016.

[46] W. W.-p. Lai, Y.-c. Chuang, and A. Y.-c. Lin. The effects and the toxicity increases caused by bicarbonate, chloride, and other water components during the uv/tio2 degradation of oxazaphosphorine drugs. *Environ Sci Pollut Res Int*, 24:14595–14604, 2017.

[47] O. Legrini, E. Oliveros, and A. M. Braun. Photochemical processes for water treatment. *Chemical Reviews*, 93:671–698, 1993.

[48] L. H. Levine, J. T. Richards, J. L. Coutts, R. Soler, F. Maxik, and R. M. Wheeler. Feasibility of ultraviolet-light-emitting diodes as an alternative light source for photocatalysis. *Journal of the Air Waste Management Association*, 61:932–940, 2011.

[49] G. Li, L. Lv, H. Fan, J. Ma, Y. Li, Y. Wan, and X. S. Zhao. Effect of the agglomeration of tio2 nanoparticles on their photocatalytic performance in the aqueous phase. *Journal of Colloid and Interface Science*, 348:342–347, 2010.

[50] W. Liu, S. A. Andrews, M. I. Stefan, and J. R. Bolton. Optimal methods for quenching h2o2 residuals prior to ufc testing. *Water Research*, 37:3697–3703, 2003.

[51] M. Martin-Somer, C. Pablos, R. van Grieken, and J. Marugan. Influence of light distribution on the performance of photocatalytic reactors: Led vs mercury lamps. *Applied Catalysis B: Environmental*, 215:1–7, 2017.

[52] R. Matta, K. Hanna, T. Kone, and S. Chiron. Oxidation of 2,4,6-trinitrotoluene in the presence of different iron-bearing minerals at neutral ph. *Chemical Engineering Journal*, 144:453–458, 2008.

[53] S. Miralles-Cuevas, D. Darowna, A. Wanag, S. Mozia, S. Malato, and I. Oller. Comparison of uv/h2o2, uv/s2o82−, solar/fe(ii)/h2o2 and solar/fe(ii)/s2o82− at pilot plant scale for the elimination of micro-contaminants in natural water: An economic assessment. *Chemical Engineering Journal, Intensification of Photocatalytic Processes for Niche Applications in the Area of Water, Wastewater and Air Treatment*, 310:514–524, 2017.

[54] R. Molinari, P. Argurio, and L. Palmisano. 7-photocatalytic membrane reactors for water treatment. *Advances in Membrane Technologies for Water Treatment*, pages 205–238, 2015.

[55] S. Mozia. Photocatalytic membrane reactors (pmrs) in water and wastewater treatment. a review. *Separation and Purification Technology*, 73:71–91, 2010.

[56] S. Mozia, K. Szymanski, B. Michalkiewicz, B. Tryba, M. Toyoda, and A. W. Morawski. Effect of process parameters on fouling and stability of mf/uf tio2 membranes in a photocatalytic membrane reactor. *Separation and Purification Technology Complete*, (142):137–148, 2015.

[57] S. Mozia, M. Tomaszewska, and A. W. Morawski. A new photocatalytic membrane reactor (pmr) for removal of azo-dye acid red 18 from water. *Applied Catalysis B: Environmental*, 59:131–137, 2005.

[58] R. Munter. Advanced oxidation processes-current status and prospects. *Proc. Estonian Acad. Sci. Chem.*, 50:59–80, 2001.

[59] S. Nussbaumer, P. Bonnabry, J.-l. Veuthey, and S. Fleury-Souverain. Analysis of anticancer drugs: A review. *Talanta*, 85:2265–2289, 2011.

[60] S. Rehman, R. Ullah, A. M. Butt, and N. D. Gohar. Strategies of making TiO_2 and zno visible light active. *Journal of Hazardous Materials*, 170:560–569, 2009.

[61] Pills Report. Pharmaceutical residues in the aquatic system : a challenge for the future. Technical report, Final Report of the European Cooperation Project PILLS, 2012.

[62] A. R. Ribeiro, O. C. Nunes, M. F. R. Pereira, and A. M. T. Silva. An overview on the advanced oxidation processes applied for the treatment of water pollutants defined in the recently launched directive 2013/39/eu. *Environment International*, 75:33–51, 2015.

[63] E. J. Rosenfeldt, K. G. Linden, S. Canonica, and Urs von Gunten. Comparison of the efficiency of oh radical formation during ozonation and the advanced oxidation processes o3/h2o2 and uv/h2o2. *Water Research*, 40(20):3695–3704, 2006.

[64] N. C. Rowney, A. C. Johnson, and R. J. Williams. Cytotoxic drugs in drinking water: a prediction and risk assessment exercise for the thames catchment in the united kingdom. *Environmental Toxicology and Chemistry*, 28:2733–2743, 2009.

[65] K. Sahel, L. Elsellami, I. Mirali, F. Dappozze, M. Bouhent, and C. Guillard. Hydrogen peroxide and photocatalysis. *Applied Catalysis B: Environmental*, 188:106–112, 2016.

[66] H. Sanderson, R. A. Brain, D. J. Johnson, C. J. Wilson, and K. R. Solomon. Toxicity classification and evaluation of four pharmaceuticals classes: antibiotics, antineoplastics, cardiovascular, and sex hormones. *Toxicology*, 203:27–40, 2004.

[67] V. C. Sarasidis, K. V. Plakas, and A. J. Karabelas. Novel water-purification hybrid processes involving in-situ regenerated activated carbon, membrane separation and advanced oxidation. *Chemical Engineering Journal*, 328:1153–1163, 2017.

[68] V. C. Sarasidis, K. V. Plakas, S. I. Patsios, and A. J. Karabelas. Investigation of diclofenac degradation in a continuous photo-catalytic membrane reactor. influence of operating parameters. *Chemical Engineering Journal*, 239:299–311, 2014.

[69] K. Song, M. Mohseni, and F. Taghipour. Application of ultraviolet light-emitting diodes (uv-leds) for water disinfection: A review. *Water Research*, 94:341–349, 2016.

[70] J. G. Speight. *Chemical Transformations in the Environment, in: Environmental Organic Chemistry for Engineers*. Elsevier, 2017.

[71] Statista. https://www.statista.com/statistics/418067/electricity-prices-for-households-in-belgium/.

[72] The Engineering Toolbox. "pump power calculator". `https://www.engineeringtoolbox.com/pumps-power-d_505.html`.

[73] Em. Topuz, J. Traber, L. Sigg, and I. Talinli. Agglomeration of ag and tio2 nanoparticles in surface and wastewater: Role of calcium ions and of organic carbon fractions. *Environmental Pollution*, 204:313–323, 2015.

[74] Cancer Research UK. "worldwide cancer statistics". http://www.cancerresearchuk.org/health-professional/cancer-statistics/worldwide-cancer.

[75] Y. Wang, F. Roddick, and L. Fan. Direct and indirect photolysis of seven micropollutants in secondary effluent from a wastewater lagoon. *Chemosphere*, 185:297–308, 2017.

[76] B. E. Watt, A. T. Proudfoot, and J. A. Vale. Hydrogen peroxide poisoning. *Toxicol Rev*, 23:51–57, 2004.

[77] J. Yu, C. Yu, K.-p. Leung J., Ho M., Cheng W., Zhao B., and Zhao X. Effects of acidic and basic hydrolysis catalysts on the photocatalytic activity and microstructures of bimodal mesoporous titania. *Journal of Catalysis*, 217:69–78, 2003.

[78] X. Zheng, Z.-p. Shen, L. Shi, R. Cheng, and D.-h. Yuan. Photocatalytic membrane reactors (pmrs) in water treatment: Configurations and influencing factors. *Catalysts*, 7:224, 2017.

Rue Archimède, 1 bte L6.11.01, 1348 Louvain-la-Neuve **www.uclouvain.be/epl**